

Dynamical downscaling of wind shear: Observational analysis and comparison of MM5 and WRF mesoscale model performance

Prepared by: Kristian Horvath

Type: Report

Date: 02/28/2013

Project: Wind Energy Monitoring and Numerical Model Validation in Nevada (NREL)

Period of work: 02/16/2013 – 02/28/2013

Contents

<i>I. Introduction</i>	2
<i>II. Observational analysis</i>	2
<i>III. Preliminary analysis of mesoscale models performance in physical space</i>	24
<i>IV. Further work</i>	30

References

I. Introduction

Regional/mesoscale models currently provide reliable wind power density products. Besides the traditional use in numerical weather prediction, this type of model is often used for regional wind resource estimates, owing to the low spatial and temporal representativeness of routine measurements. While wind speed measurements and mesoscale model accuracy in simulating wind speeds has been extensively studied (e.g. for central Nevada see Horvath, K. et al., 2012), analysis, modeling and forecasting of wind shear has received much less attention. Yet, wind shear is very important for wind power plant performance as well as loads on the turbines. Therefore, accurate representation of wind shear in models used for dynamical downscaling and in numerical weather prediction is essential for reducing the meteorological uncertainties related to wind energy utilization.

Furthermore, in many applied scientific disciplines including wind engineering, it is often considered that the higher resolution the better, i.e. that increased horizontal resolution of the model yields more accurate results. However, the gain in forecast accuracy with increased horizontal resolution is not always straightforward.

The principal questions to be addressed in this study are:

1. What is the accuracy of the sub-kilometer dynamical downscaling of near-surface wind speed and wind shear over complex terrain using the WRF and MM5 mesoscale models?
2. Does a uniform mesh refinement in mesoscale models uniformly enhance the accuracy of the near-surface wind shear estimates, and what is the grid spacing required for obtaining a reliable estimate of near-surface wind shear over complex terrain? How equivalent are the momentbased and spectral verification metrics in assessing the model's performance and the potential accuracy improvement with increasing the horizontal resolution?
3. What are the strengths and weaknesses of dynamical downscaling of wind shear using mesoscale models and what are the rationales and/or hypothesis that can be attributed to the sources of errors?

II. Observational analysis

The observations used in this study are located in west-central Nevada, approximately 100 km east of the northern tip of the Inyo Mountain Range of the Sierra Nevada Mountains. The region is a basin and range province, characterized by several mostly north-south oriented narrow mountain ranges. Secondary mountain ranges in the area reach elevations as high as 3000 m, and on average stand about 1500 m over the surrounding plains. The large-scale terrain tilt is greatest toward the south. The climate is generally semiarid and the vegetation is sparse. The land-cover around the stations is very uniform with isolated bushes up to 1-m height. The aridity of the region leads to a high Bowen ratio and large diurnal variations in the sensible heating in the warm part of the year. Together with the orographic features of the region, these properties are highly conducive to the onset and maintenance of thermally driven diurnal circulations. In summer, the entire region is typically characterized by deep and extremely well-mixed daytime convective boundary layers and a strong stably stratified nocturnal boundary layer with near-surface inversions. In winter, however, the atmospheric processes are mainly determined by the passages of frontal systems coming from the Pacific.

The observational analysis in this study uses measurements at 50-m towers set up in the focal area. The observed wind regime in west-central Nevada as inferred from the network of four 50-m

meteorological towers (geographical locations shown in Figure 1) for the period September 2003–March 2008 was documented in Belu and Koracin (2009). Additional details on the observed properties of wind speed are presented in Horvath et al. (2012). These towers were equipped with RM Young 05103 four blade helicoid propeller anemometers at 10 m, 20 m, 30 m, 40 m, and 50 m above ground level (AGL). Each anemometer was individually calibrated, with accuracy within $\pm 0.3 \text{ ms}^{-1}$ or 1% of the reading. At the top of the 50-m wind towers two arms with anemometers were mounted opposite to each other with azimuths of 255° and 75° . The differences in the mean wind speeds between the two sensors at the same height were on average much smaller than the sensor accuracy limit, though individually they might have occasionally reached the sensor accuracy limit individually. For example, in July 2007 the mean difference between the two sensors averaged over all towers was approximately 0.025 ms^{-1} . Therefore, the average effect of the wind towers on the data we used for analysis and verification may be considered small. The data were collected at 1 Hz frequency, quality controlled and interpolated to fill the missing data (less than 3%). For the analysis in this paper, we used data from ENE-facing sensor. More information on quality control is found in Belu and Koracin [2009].

The observational analysis was performed for four 50-m wind towers in west-central Nevada, that will be used for analysis of observations, development of modeling strategies and development of verification tools and evaluation of the models prior to collection of newly deployed measurements within the project. Following Horvath et al., 2012, two representative periods are chosen for study: July 2007, characterized with intense diurnal flows and December 2007 characterized with weak energy of motions in diurnal spectral band. Wind shear was calculated as $\partial V/\partial z$ and in graphical presentation (unless specified otherwise) scaled with a factor of 100 - thus wind shear unit is 100 m/s^2 . Because any slight errors in the wind speed can cause considerable errors in the wind shear estimates for thin layers, wind shear is also calculated over 20 m layers. Furthermore, for wind energy assessment, typically only wind shears for heights above about 30–40m and wind speeds above about 4 m/s are evaluated. In the initial phase of the analysis, we will analyze the wind shear at lower heights and lower wind speeds, to help understand the properties of wind regime in the area (e.g. type and depth of flows, lower boundary effects of terrain and roughness, etc..) and interpret both observations and modelling results. Finally, in this very report, we focus only on observational analysis for July 2007.



Figure 1: Locations of the wind towers used in this study: 50-m wind towers are Tonopah 24N, Kingston 14SW, Luning 5N and Luning 7W. Stone Cabin is 80-m tower.

Due to surface drag, positive mean wind shear (increasing winds) are typically found in the lowest 50 m above ground. Wind shear is typically stronger at 10 m level than somewhat above. However, in case of shallow circulations (such as katabatic flows with low-level jets at 10 m or 20 m AGL) wind shear in the lowest 50 m can be negative. Therefore, mean wind shear over a longer period is expectedly positive, except in climates governed by very shallow circulations.

Mean wind speed profiles show a general increase with height at all analyzed wind towers (Fig. 2). For all wind towers wind speed at 50 m is higher than wind speed at 20 m, which is higher than wind speed at 10 m height. However, between other levels wind speed does not necessarily increase with height. Mean wind shear at all 4 analyzed wind towers is the strongest between two levels adjacent to the ground (Fig 3). At 10 m vertical separation for wind shear calculation, mean wind shear during the analyzed period does not necessarily monotonously decrease with height. As inferred by the analysis, negative wind shear at low-levels may exist not only for sporadic episodes but also on average (Figure 3, top panel). For example, Tonopah shows negative mean wind shear between 20m and 30m AGL while Luning7W shows negative wind shear between 40m and 50m AGL. Additionally Luning 5N shows smaller (positive) wind shear between 20 m and 30 m heights than between 30 m and 40 m heights. The negative wind shear at certain sub-region in the lowest 50 m AGL was found also in Belu and Koracin (2009) on average for the entire period September 2003–March 2008. First, one of the reasons for negative wind shear at Luning 7W and Tonopah during summer may be the frequent presence of shallow nocturnal circulations. Second, it should be noted again that calculating wind shear with 10 m vertical separation is very sensitive to any potential errors in measured data. At 20 m vertical separation, data shows no negative mean wind shear and mean wind shear generally shows more monotonous decrease with height. The only exception is found for the wind tower at Tonopah, where mean wind shear between 20 m and 40 m levels is smaller than wind shear between 30 m and 50 m levels. Note however, that mean wind shear between 10 m and 50 m level is as expected positive for all analyzed stations.

Due to existence of mean negative wind shear at two stations (calculated at 10 m vertical separation), wind measurements were quality controlled by the correlation test, which compared correlations between different pairs of levels. E.g. for Tonopah where negative wind shear is found between 20 m and 30 m levels, correlations are $corr(v_{20m}, v_{30m})=0.991$, $corr(v_{30m}, v_{40m})=0.995$ and $corr(v_{20m}, v_{40m})=0.985$. This shows that correlation between wind speed at 20 m AGL and wind speed at 40 m AGL is smaller than correlations between the adjacent levels. This fact excludes potential observational deficiencies, such as what would be in case that correlation between winds at 20m and 40m AGL is higher than correlation between the adjacent levels. While this test is not a guarantee that the specific sensor at Tonopah at 30 m height works properly and that it does not read too low, it appears that the mean wind shear shows considerable deviations compared to expected decrease with height on several wind towers. Therefore, non-monotonous change of mean wind shear with height seems to be a property of the wind regime in the area. At this moment, it is not clear what the reasons for this wind shear behavior are.

Due to the importance of diurnal flows in summer, mean vertical wind shear was calculated also for nighttime and daytime periods separately (Figures 4 and 5). For both daytime and nighttime, as well as for mean values during the entire month, wind shear is the strongest between two levels adjacent to the ground. During the daytime, with shear between 30 m and 40 m is stronger than between 20 m and 30 m for two wind towers, while during the nighttime this is found for all stations except for Luning7W. During daytime, using 20 m vertical separation (Fig. 4b), wind shear decreases with height for all

stations except for Tonopah. During nighttime, however, wind shear between 30 m and 50 m is stronger than wind shear between 20 m and 40 m heights. This suggests that wind shear during the night generally does not change monotonously with height, and point to potential presence of shallow nocturnal flows.

We further analyze time series of wind shear for daytime and nighttime periods. Time series of wind shear for Tonopah is shown in Figure 6, and reveals that although the mean values are similar during daytime and nighttime wind shear variability is much larger during nighttime (Fig. 6). Similar is found for Kingston (Figure 7), Luning 5N (Figure 8) and Luning 7W (Figure 9), being the universal founding of the wind shear climate at analyzed stations. This suggests wind shear distributions are quite different during daytime and nighttime, which will be further analyzed in more detail. Finally, maximal wind shear values (both positive and negative) are much more frequent during the night, likely due to weaker and more stratiform (less mixed) winds in the nocturnal planetary boundary layer.

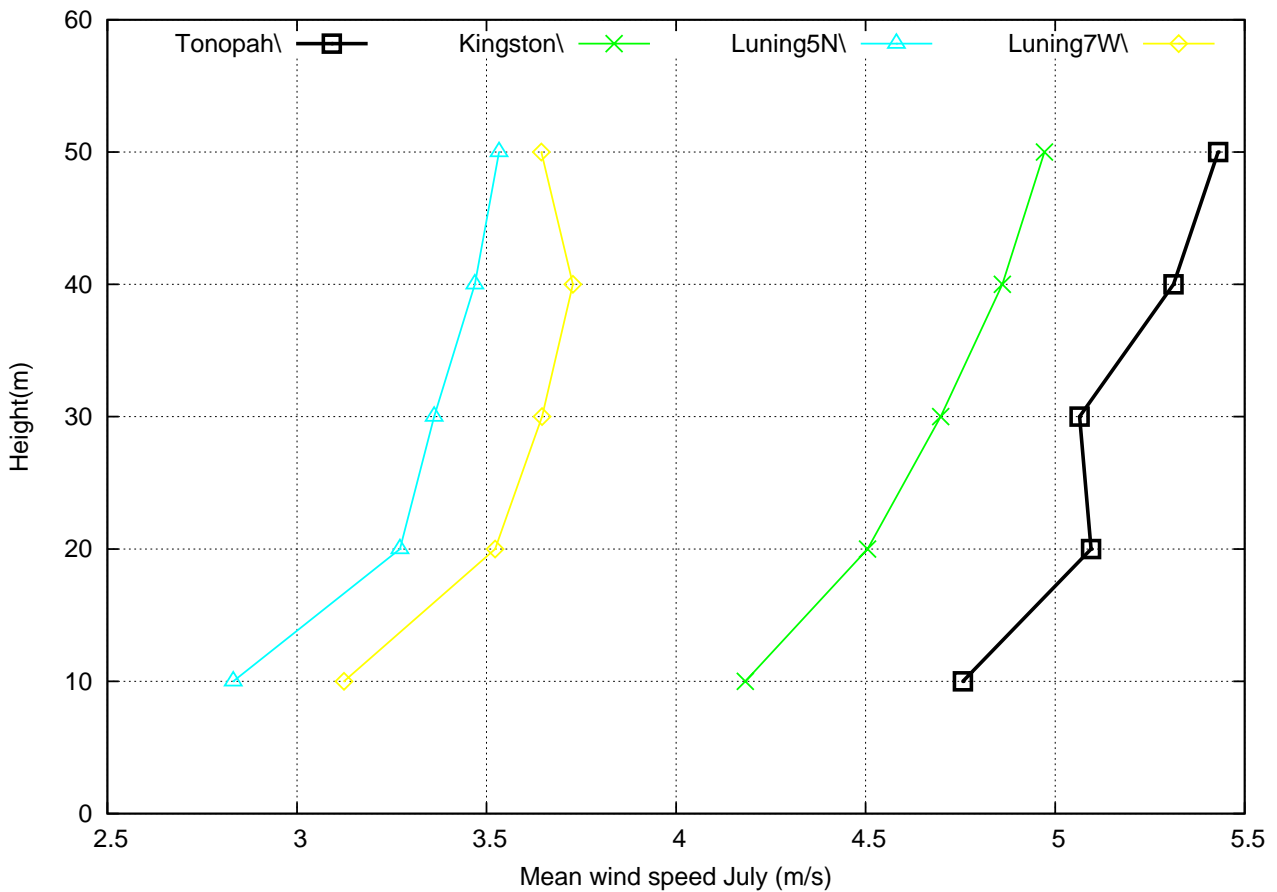


Figure 2: Measured mean wind speed (m/s) for July 2007 at stations Tonopah, Kingston, Luning5N and Luning7W.

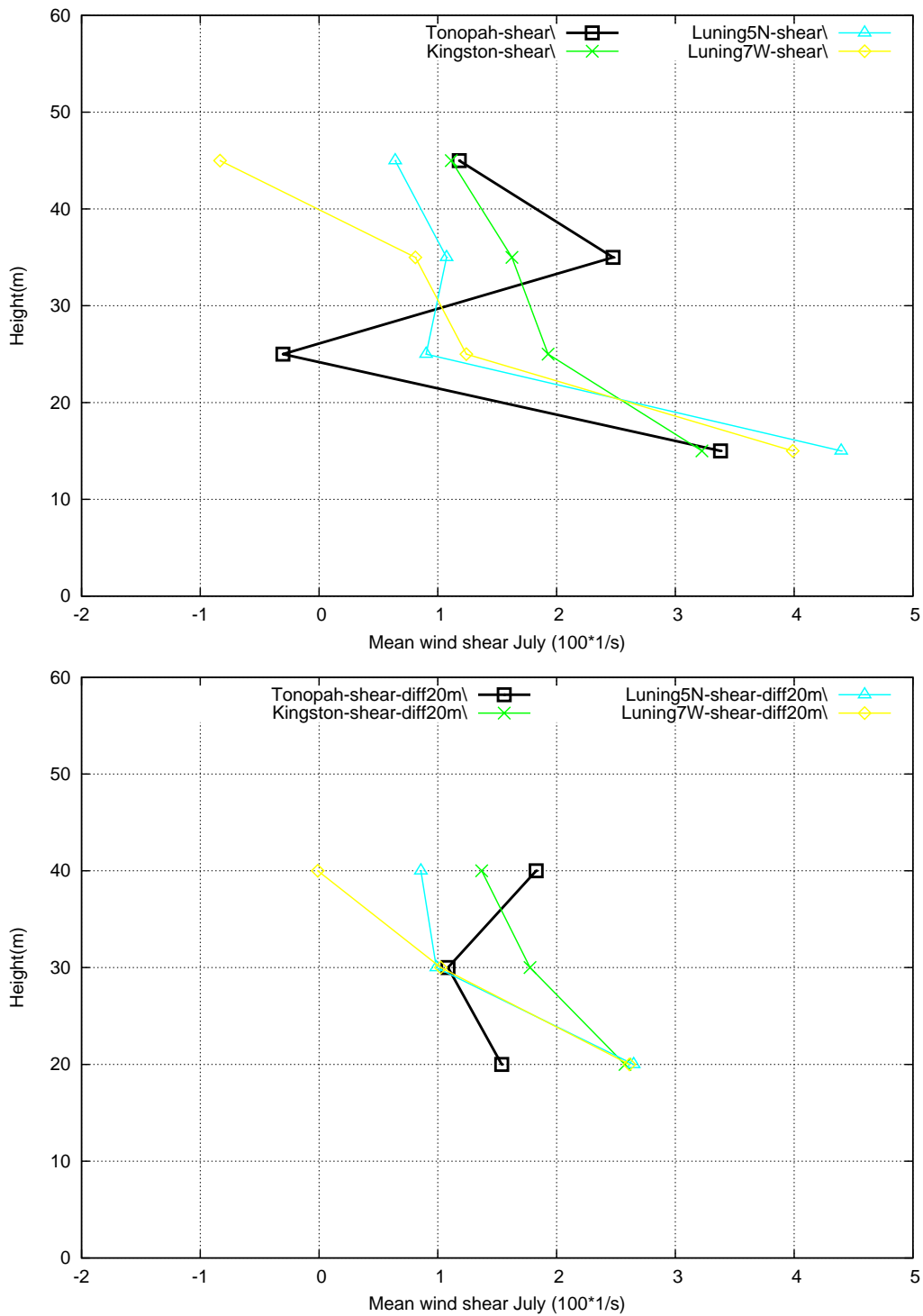


Figure 3: Measured mean wind shear for July 2007 at stations Tonopah, Kingston, Luning5N and Luning7W for 10 m vertical separation - layers 50-40, 40-30, 30-20, 20-10 (top) and for 20 m vertical separation – layers 50-30, 40-20, 30-10 (bottom).

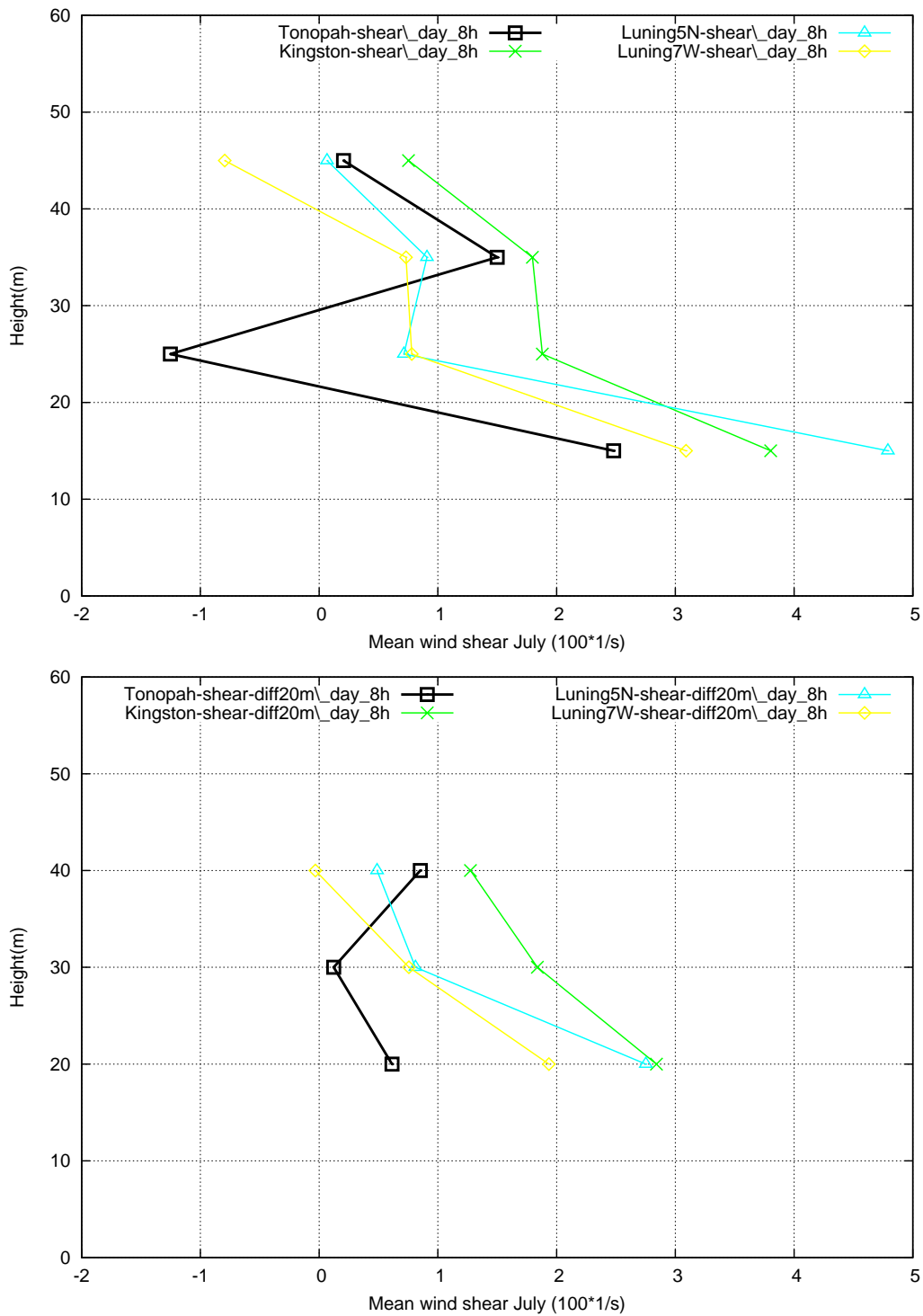


Figure 4: Measured mean wind shear during daytime for July 2007 at stations Tonopah, Kingston, Luning5N and Luning7W for 10 m vertical separation - layers 50-40, 40-30, 30-20, 20-10 (top) and for 20 m vertical separation – layers 50-30, 40-20, 30-10 (bottom).

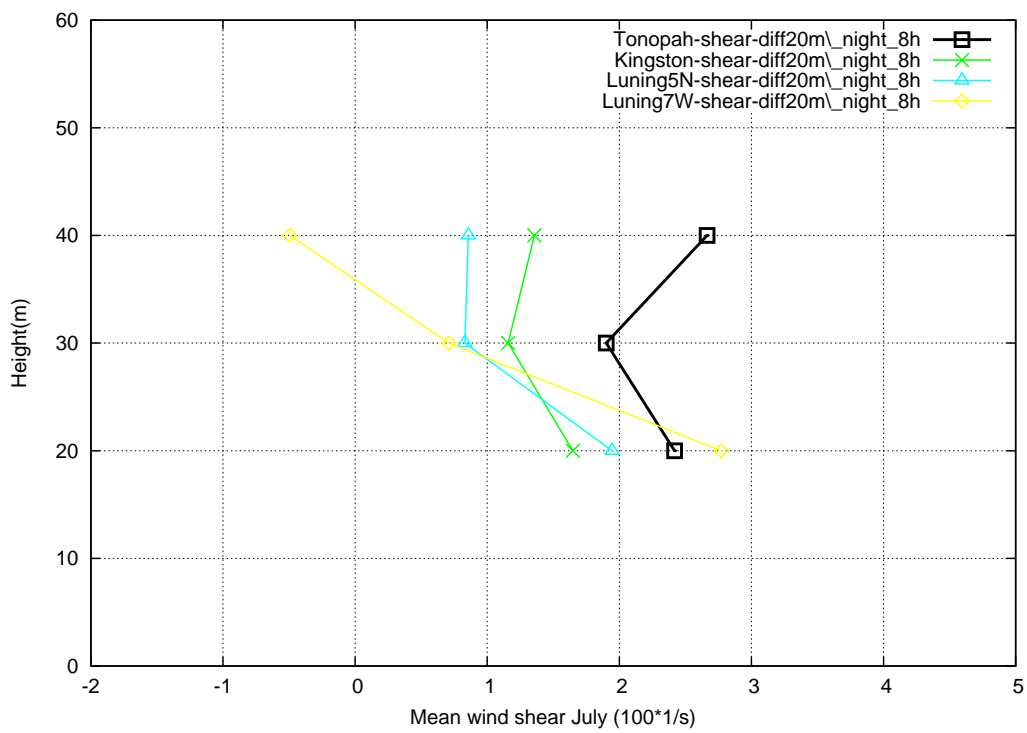
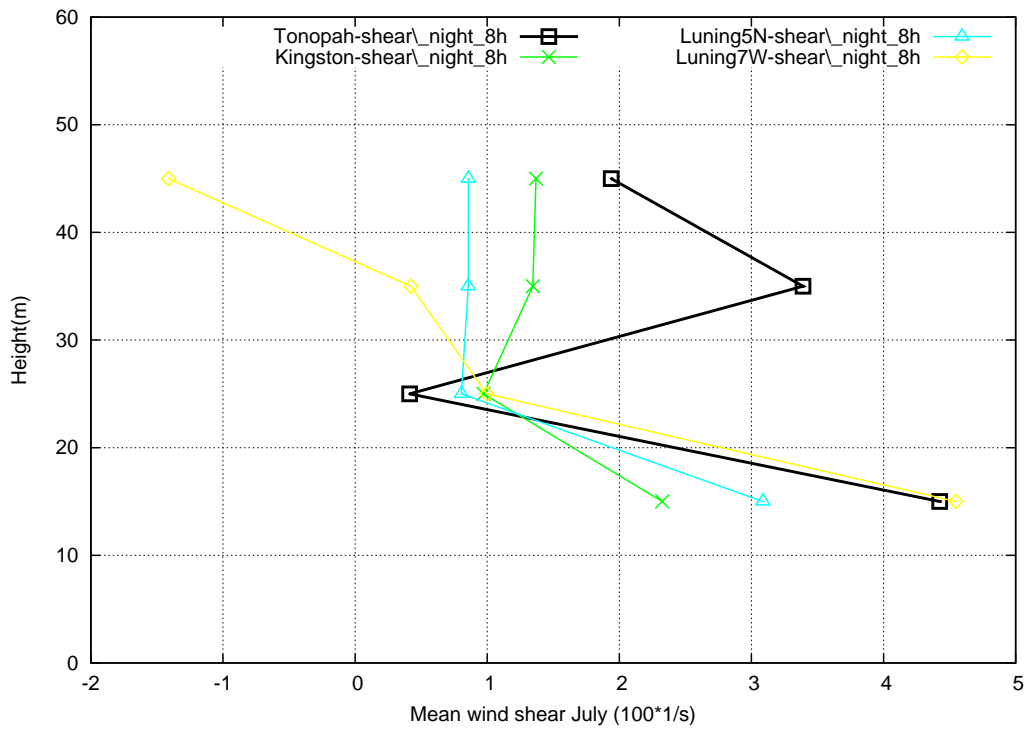


Figure 5: Measured mean wind shear during daytime for July 2007 at stations Tonopah, Kingston, Luning5N and Luning7W for 10 m vertical separation - layers 50-40, 40-30, 30-20, 20-10 (top) and for 20 m vertical separation – layers 50-30, 40-20, 30-10 (bottom).

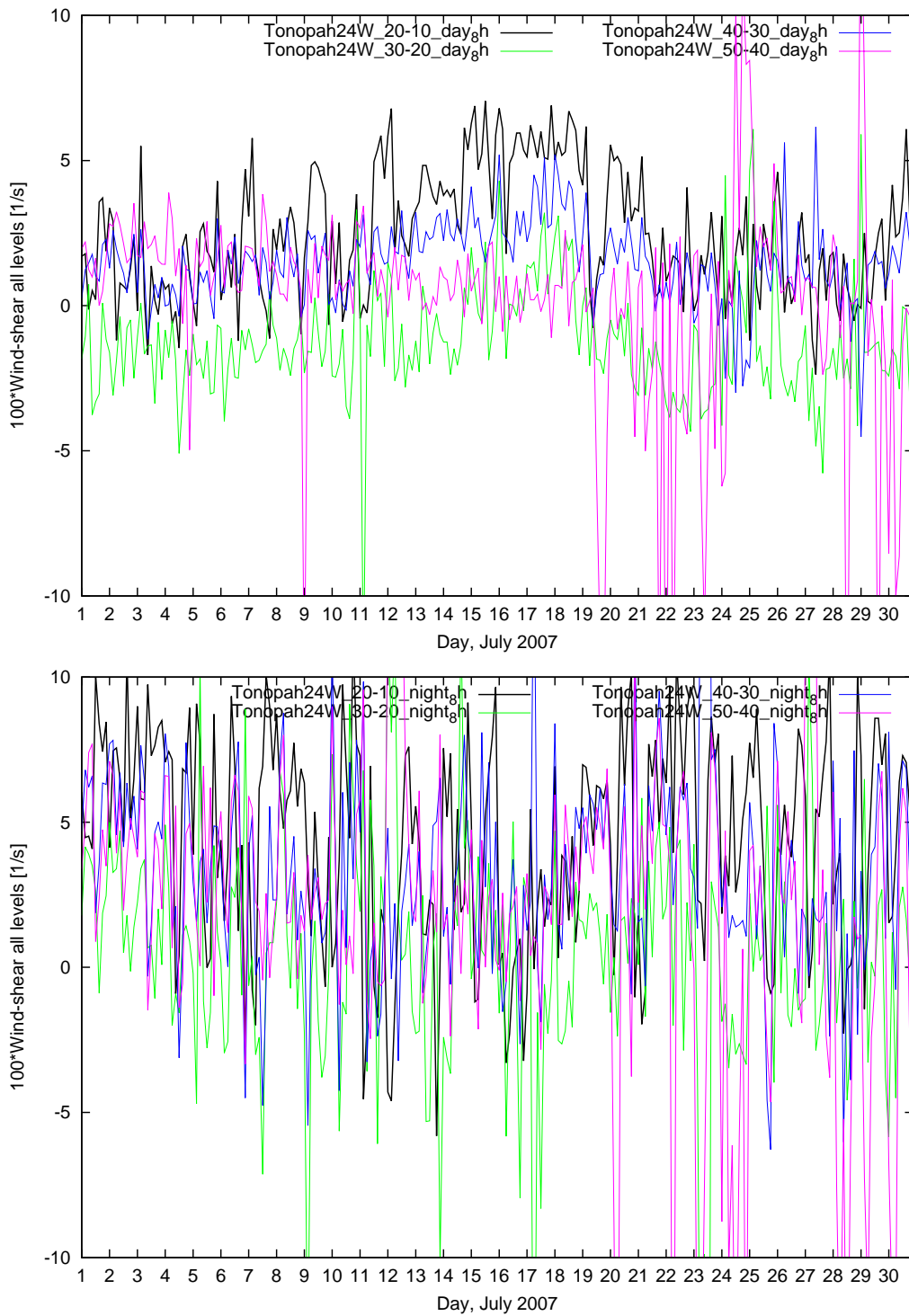


Figure 6: Time series of measured wind shear during daytime (top) and nighttime (bottom) for July 2007 at station Tonopah 24W.

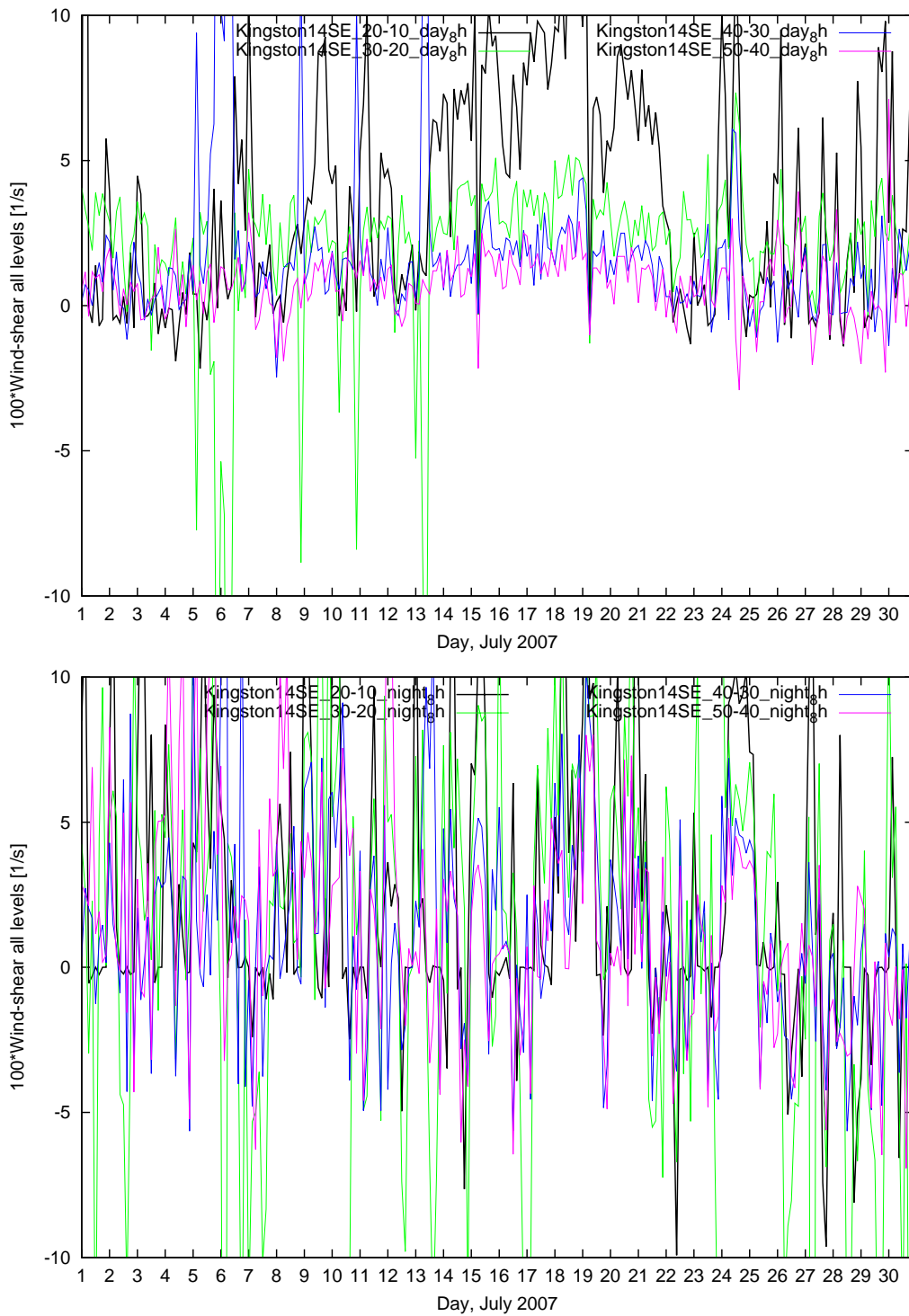


Figure 7: Time series of measured wind shear during daytime (top) and nighttime (bottom) for July 2007 at station Kingston.

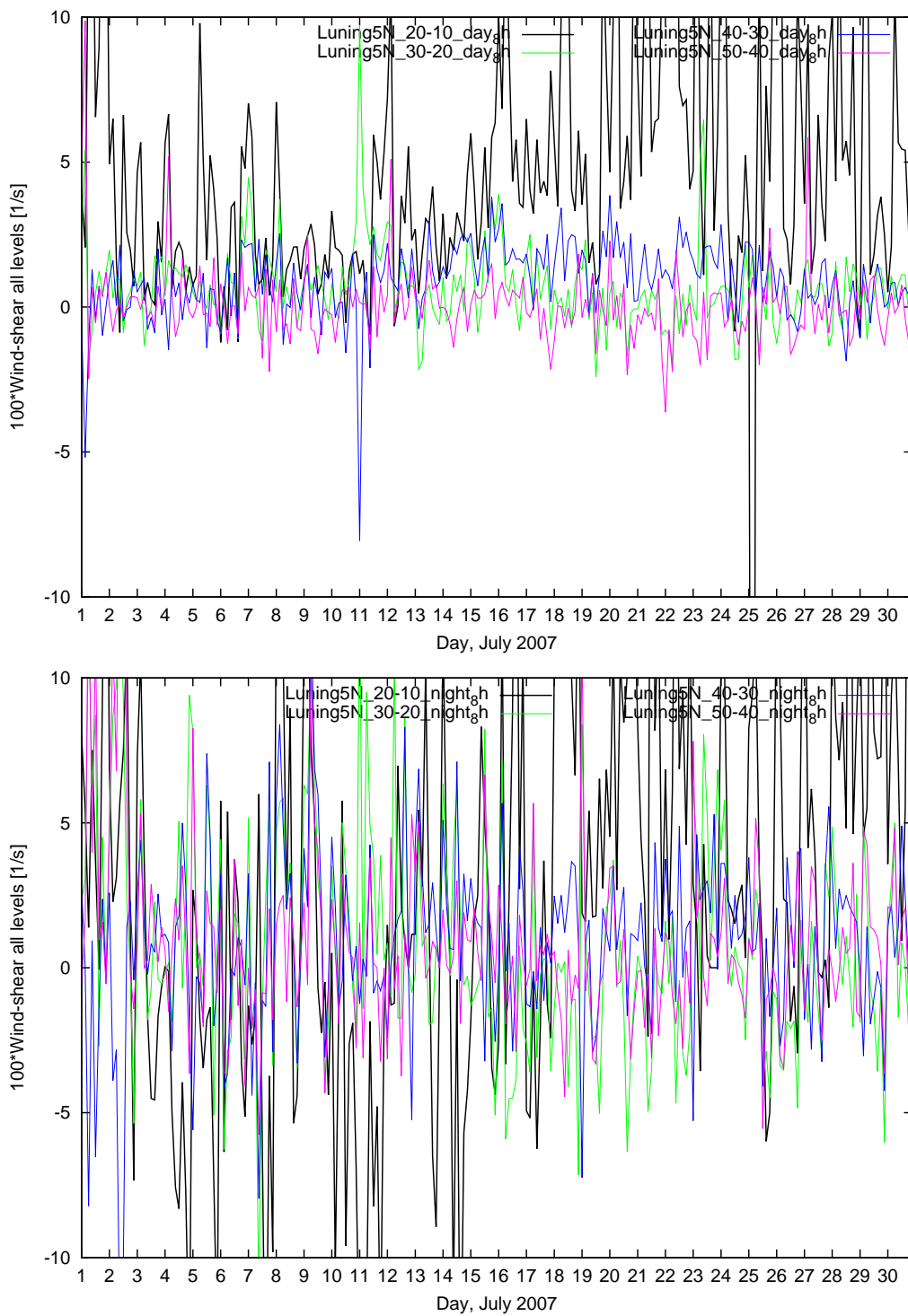


Figure 8: Time series of measured wind shear during daytime (top) and nighttime (bottom) for July 2007 at station Luning 5N.

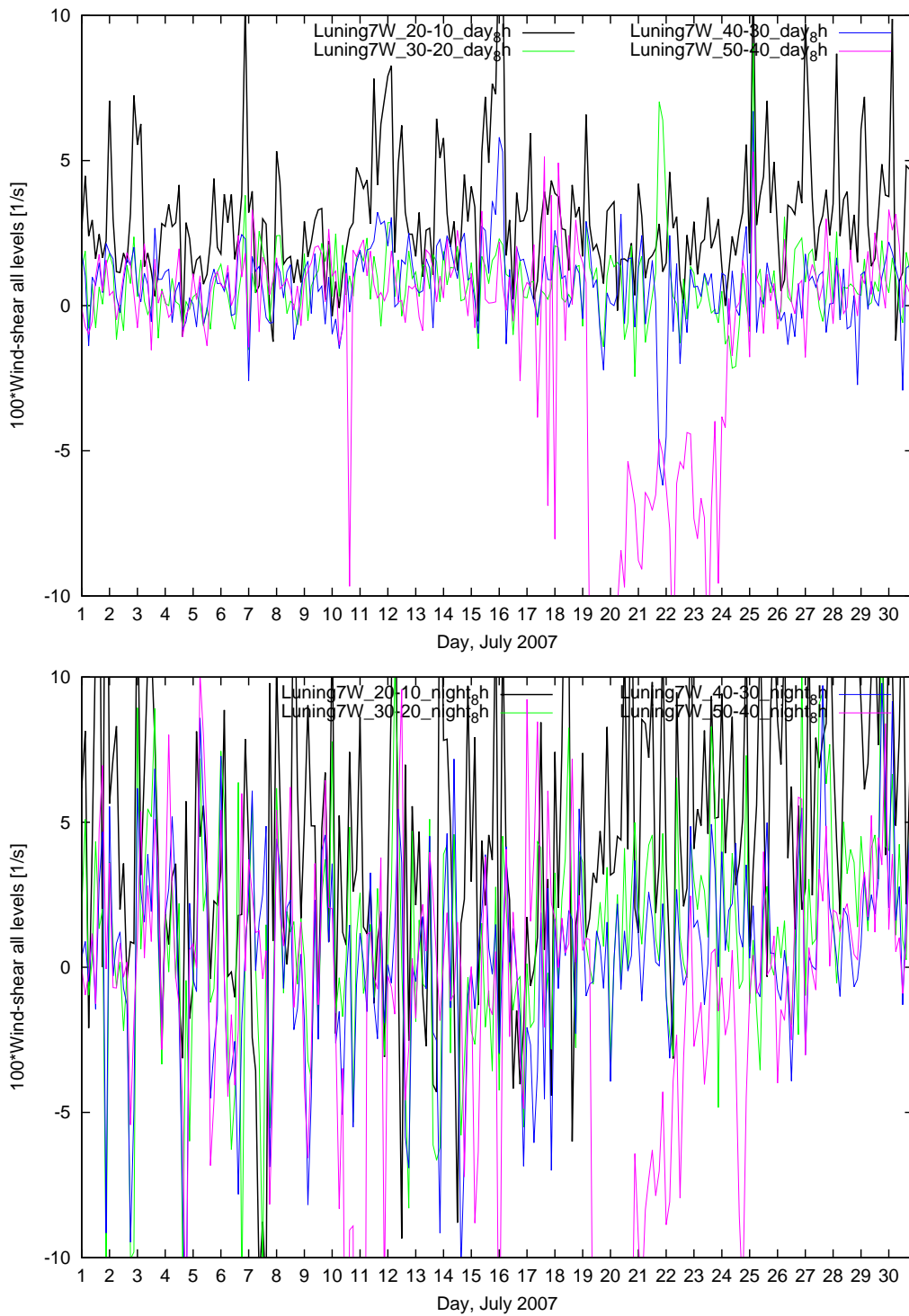


Figure 9: Time series of measured wind shear during daytime (top) and nighttime (bottom) for July 2007 at station Luning 7W.

Wind shear between 20 m and 10 m AGL was studied by means of scatter plots versus wind speed at 10 m AGL (Figures 10-13). During daytime, wind shear grows with wind speed and the relationship is almost linear for all the wind towers. Negative wind shear is generally found for wind speeds lower than 5 m/s although there are occasional exceptions. In contrast, during nighttime all wind towers show quite irregular non-linear relationship between wind shear and wind speed, with a much higher scatter. For stations Luning 5N and Luning 7W and for nocturnal winds higher than 5 m/s stronger winds are related to stronger wind shear (similar to daytime winds), but for weaker nocturnal winds large scatter suggests no clear relationship. For station Tonopah, wind shear grows with wind speed during the night for winds of up to 5 m/s and then decreases. For the few cases of the strongest nocturnal winds, wind shear is negative. For Kingston and nocturnal winds lower than 6 m/s there seems to be two wind shear regimes where wind shear grows or decreases with increasing wind speed. For Kingston and nocturnal winds higher than 5 m/s, wind shear seems to grow with increasing wind speed.

Wind shear between 50 m and 40 m AGL was studied by means of scatter plots versus wind speed at 50 m AGL (Figures 14-17). Generally, the wind shear properties regarding daytime and nighttime are reversed. Wind shear grows with wind speed more during nighttime, while the scatter remains larger during the night though. Negative wind shear is not associated only with the weaker winds such as in case of wind shear between 20 m and 10 m AGL. For Tonopah, wind shear decreases with wind speed during daytime (Figure 14) in striking contrast to wind shear properties adjacent to the ground (Figure 10) and a portion of strongest daytime winds shows negative wind shear. During nighttime however, weaker winds have more frequent negative wind shear, which is completely absent for stronger nocturnal flows. For daytime winds in Kingston (Figure 15), the growth of wind shear with wind speed is more pronounced for nocturnal winds, while daytime wind shear shows a slight tendency to grow with increasing wind speed. Wind shear at Luning 5N and Luning 7W (Figures 16 and 17) show less pronounced trends with increasing wind speed. The most apparent property of wind shear is the dominance of negative wind shear for weaker winds regardless of the period of the day.

The relationship between wind shear and wind direction was evaluated concerning the distinct properties of daytime and nocturnal flows when diurnal circulation in summer is allowed to develop that is when there is no strong synoptic forcing (Figures 18-21). It should be mentioned that wind roses for these four stations are mostly bipolar: for Tonopah dominant wind directions are NNW and SSE, for Kingston SW and NE, for Luning 5N NNW and SSE, and for Luning 7W W and E. For stations Tonopah (Figure 18) and Luning 5N (Figure 20), there is not much variability in wind shear properties with respect to wind direction. For other two stations, the variability is more evident. E.g. for Kingston (Figure 19) during daytime wind shear is stronger for daytime diurnal southerly (SW) flows than for westerly and northerly flows presumably of larger-scale origin. During nighttime, northeasterly diurnal flows have positive wind shear and ESE flows which are not of diurnal origin show mostly negative wind shear. For Luning 7W (Figure 20) wind shear during daytime does not show much sensitivity to wind direction, in contrast at nighttime when easterly flows show considerably more often negative wind shear than westerly flows which generally show positive wind shear.

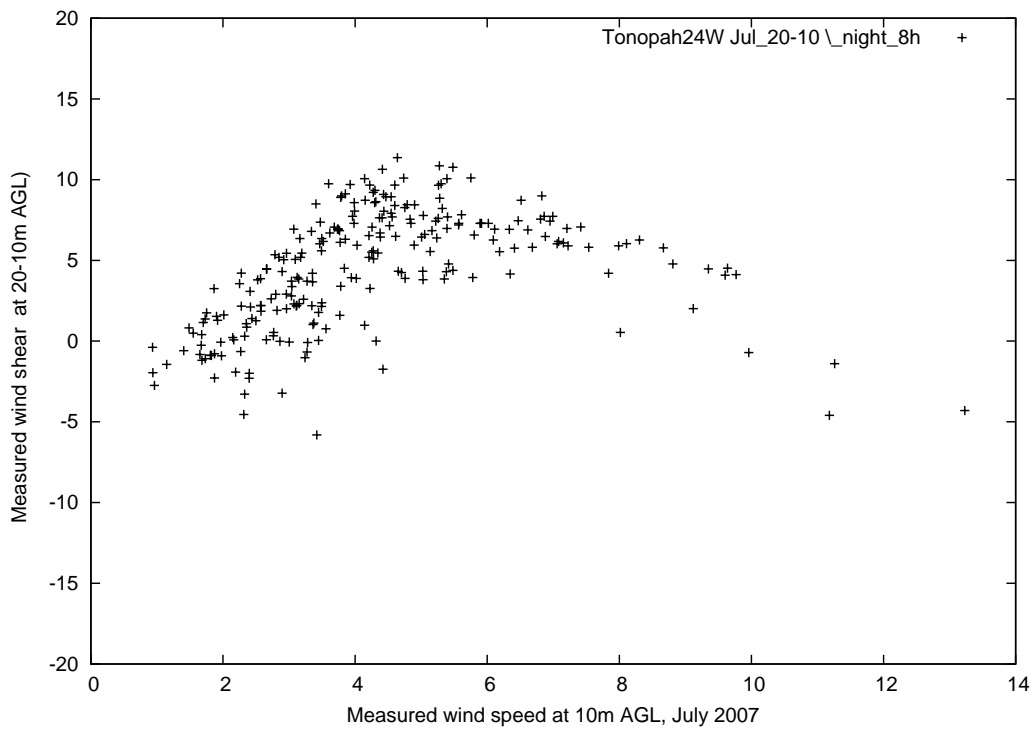
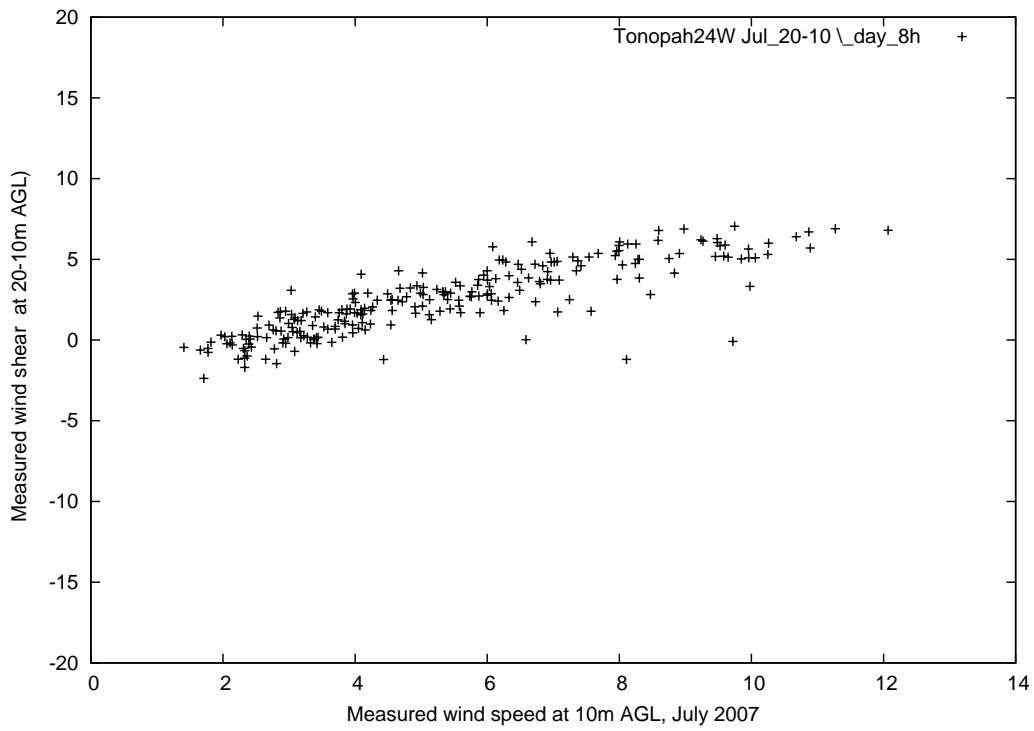


Figure 9: Scatter plots of measured wind shear between 20 m and 10 m AGL versus measured wind speed at 10 m AGL during daytime (top) and nighttime (bottom) for July 2007 at station Tonopah.

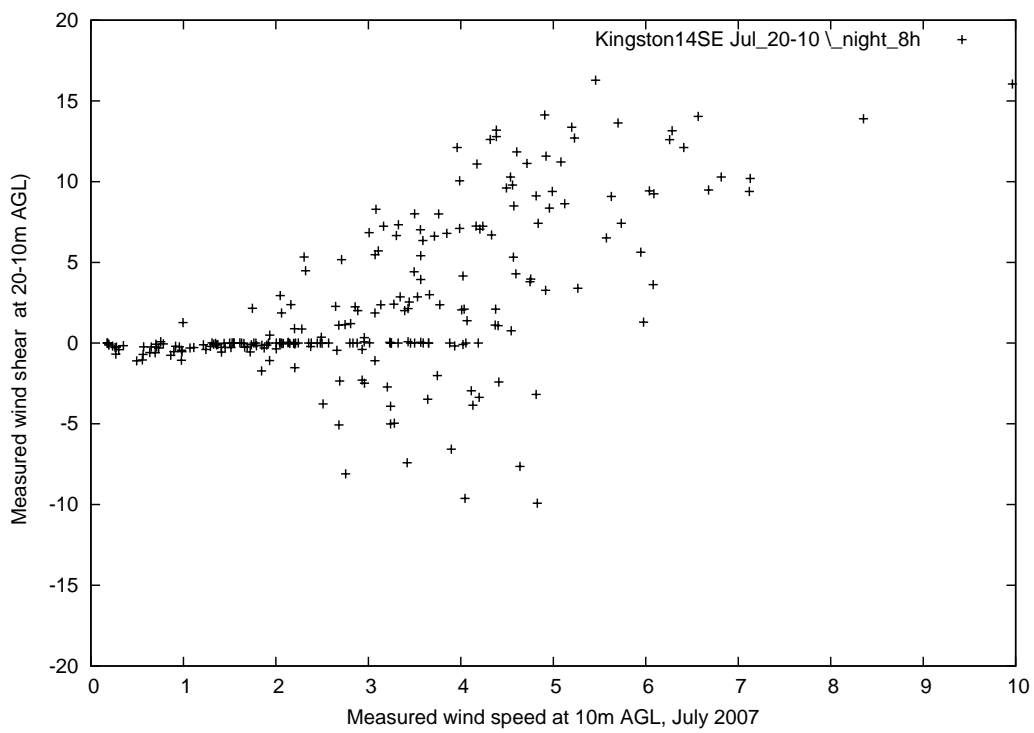
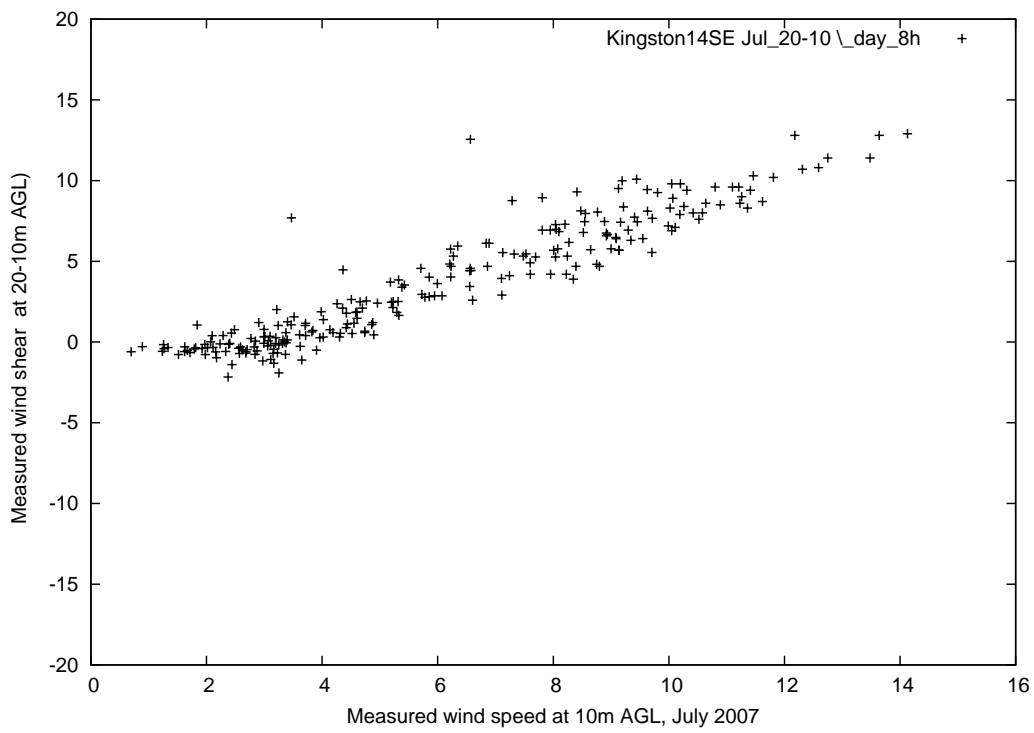


Figure 10: Scatter plots of measured wind shear between 20 m and 10 m AGL versus measured wind speed at 10 m AGL during daytime (top) and nighttime (bottom) for July 2007 at station Kingston.

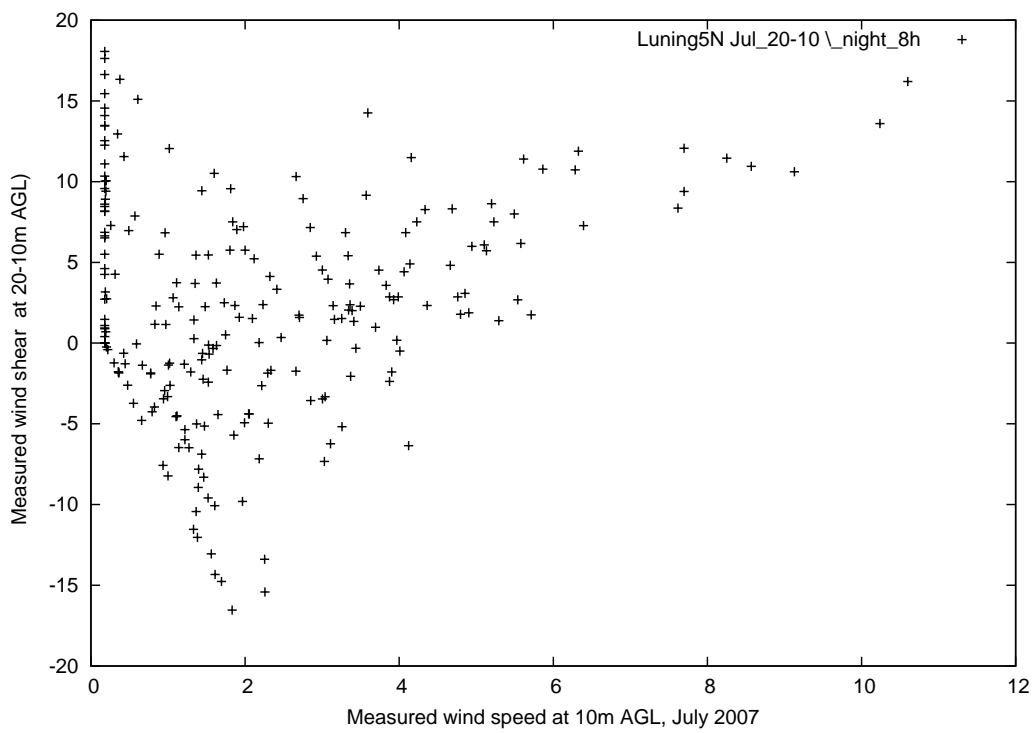
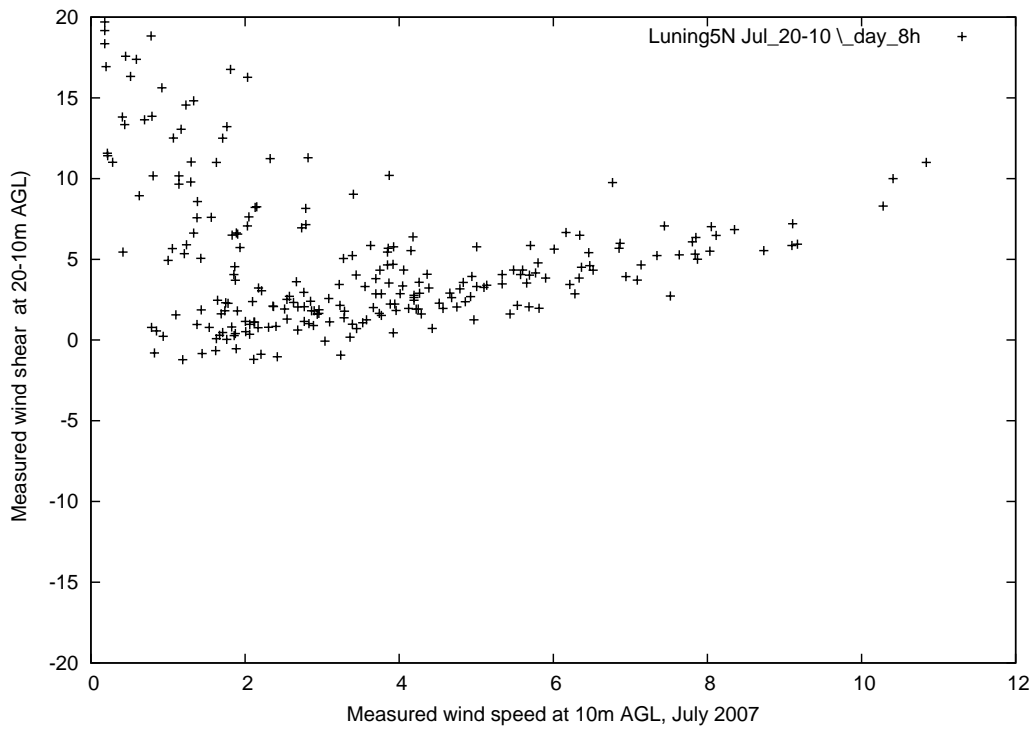


Figure 11: Scatter plots of measured wind shear between 20 m and 10 m AGL versus measured wind speed at 10 m AGL during daytime (top) and nighttime (bottom) for July 2007 at station Luning 5N.

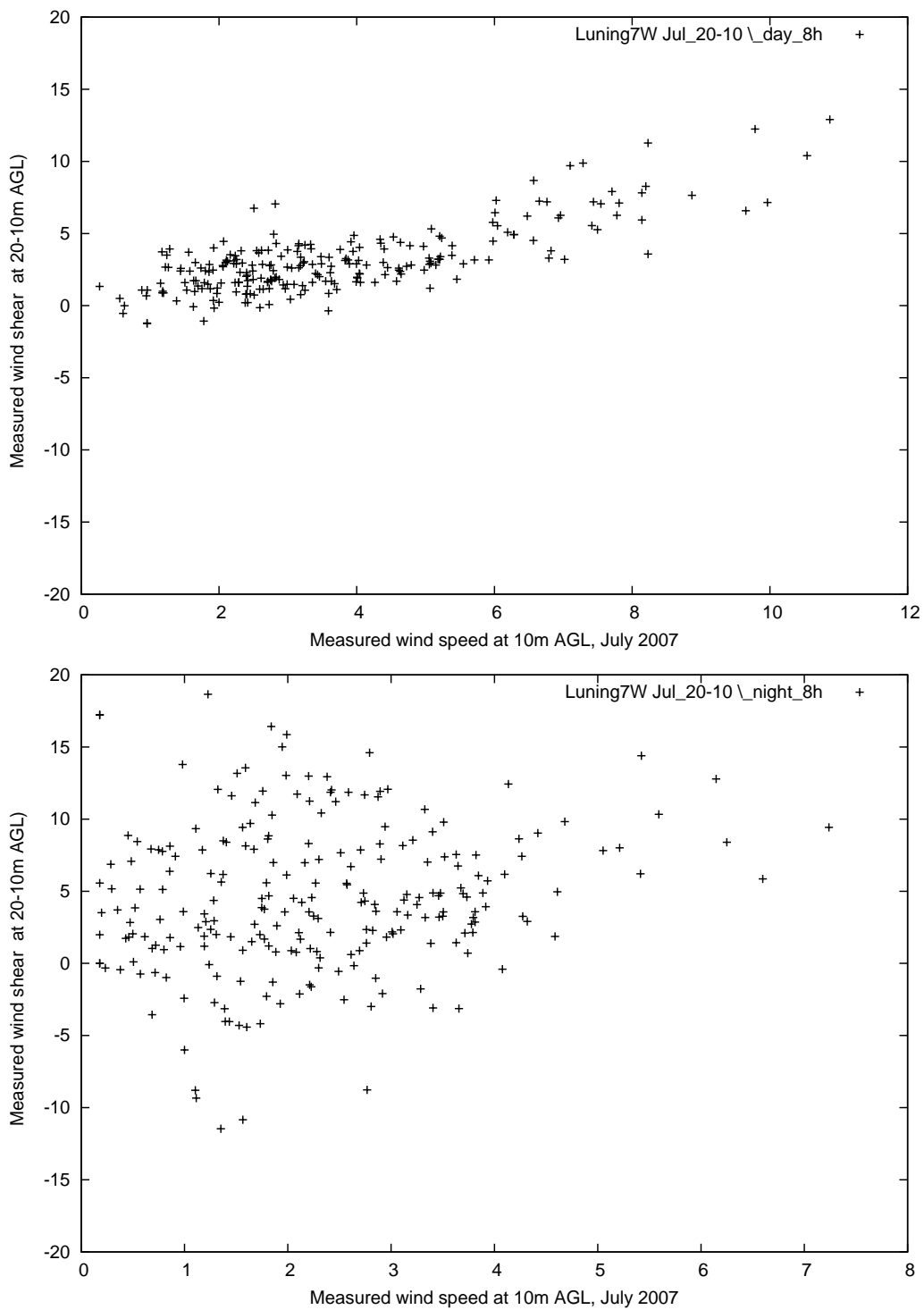


Figure 12: Scatter plots of measured wind shear between 20 m and 10 m AGL versus measured wind speed at 10 m AGL during daytime (top) and nighttime (bottom) for July 2007 at station Luning 7W.

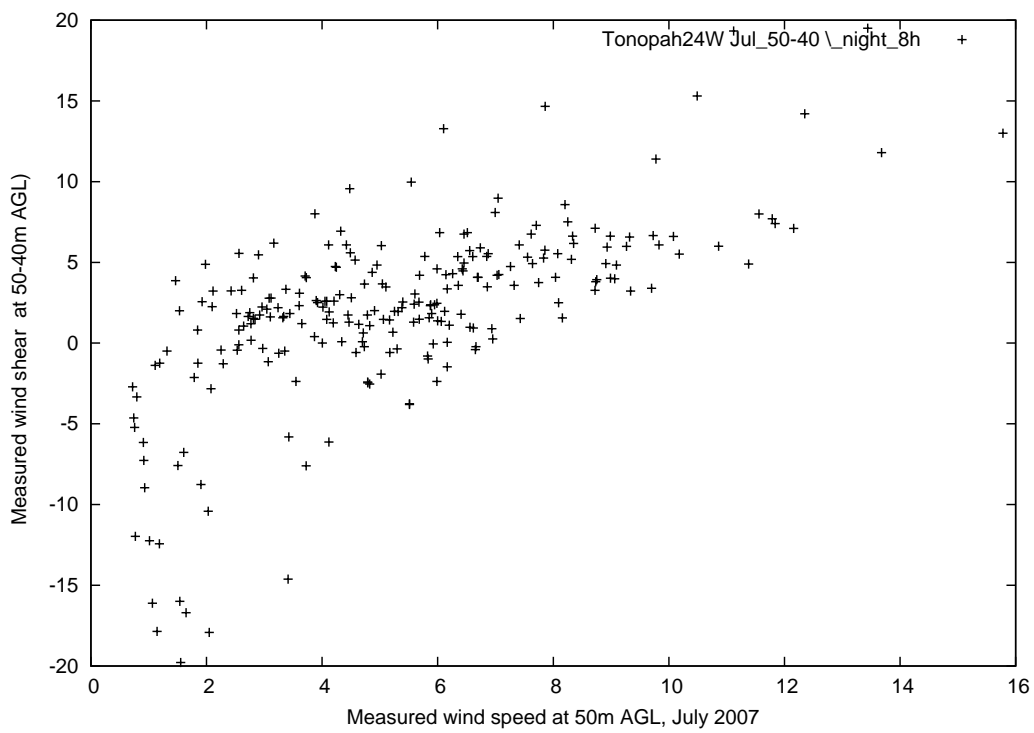
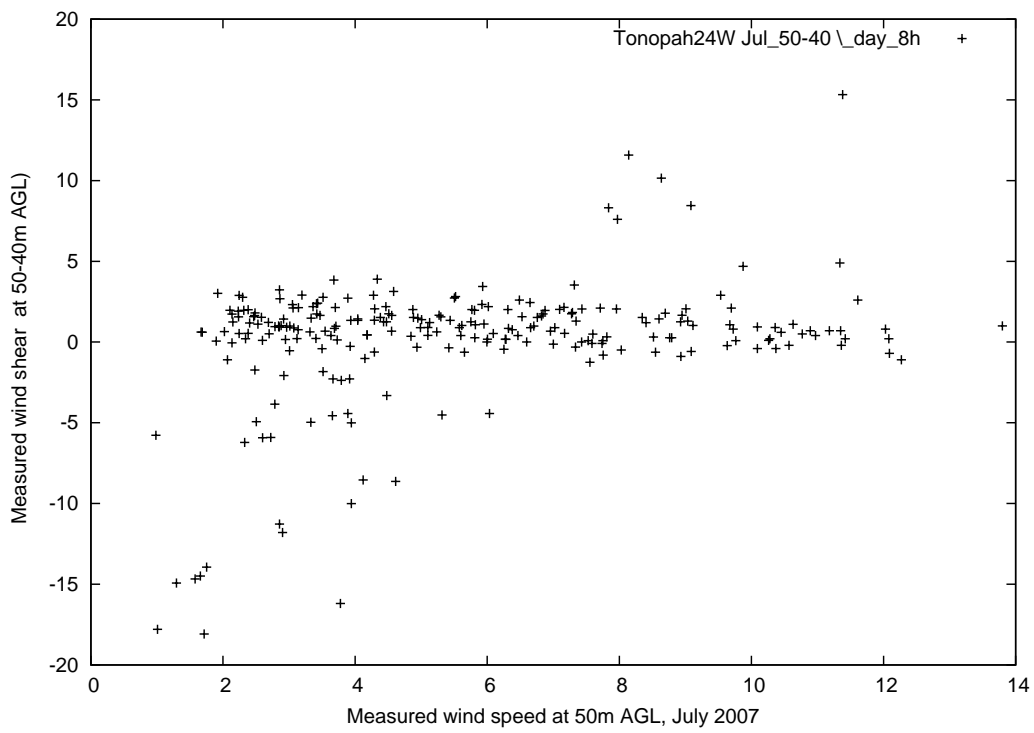


Figure 13: Scatter plots of measured wind shear between 50 m and 40 m AGL versus measured wind speed at 50 m AGL during daytime (top) and nighttime (bottom) for July 2007 at station Tonopah.

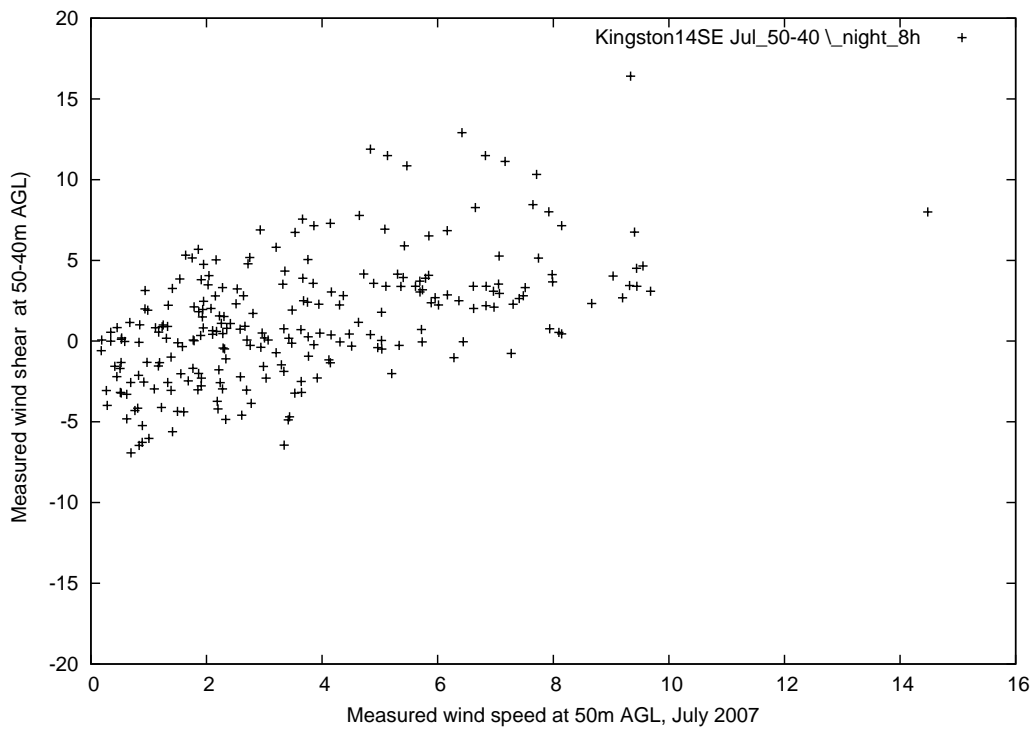
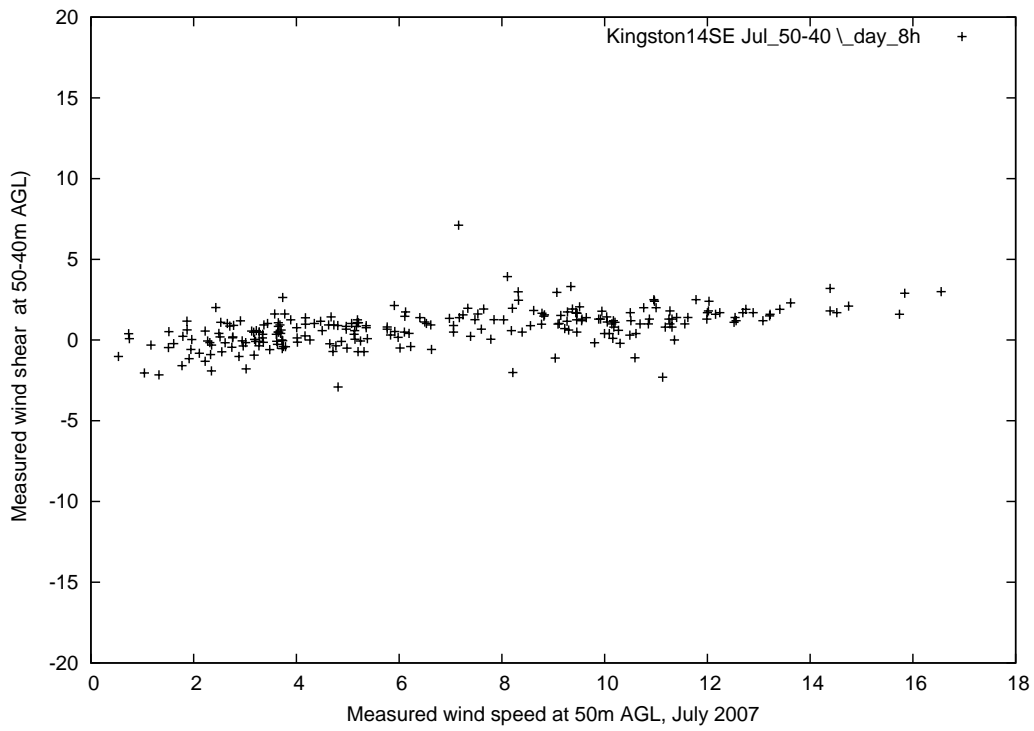


Figure 14: Scatter plots of measured wind shear between 50 m and 40 m AGL versus measured wind speed at 50 m AGL during daytime (top) and nighttime (bottom) for July 2007 at station Kingston.

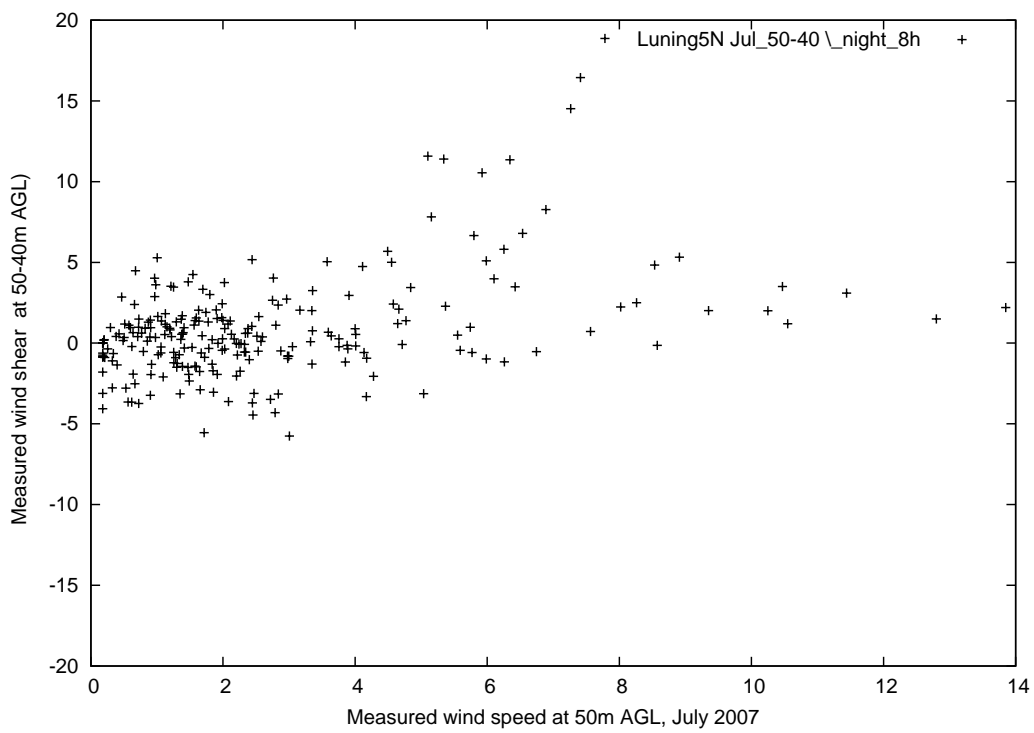
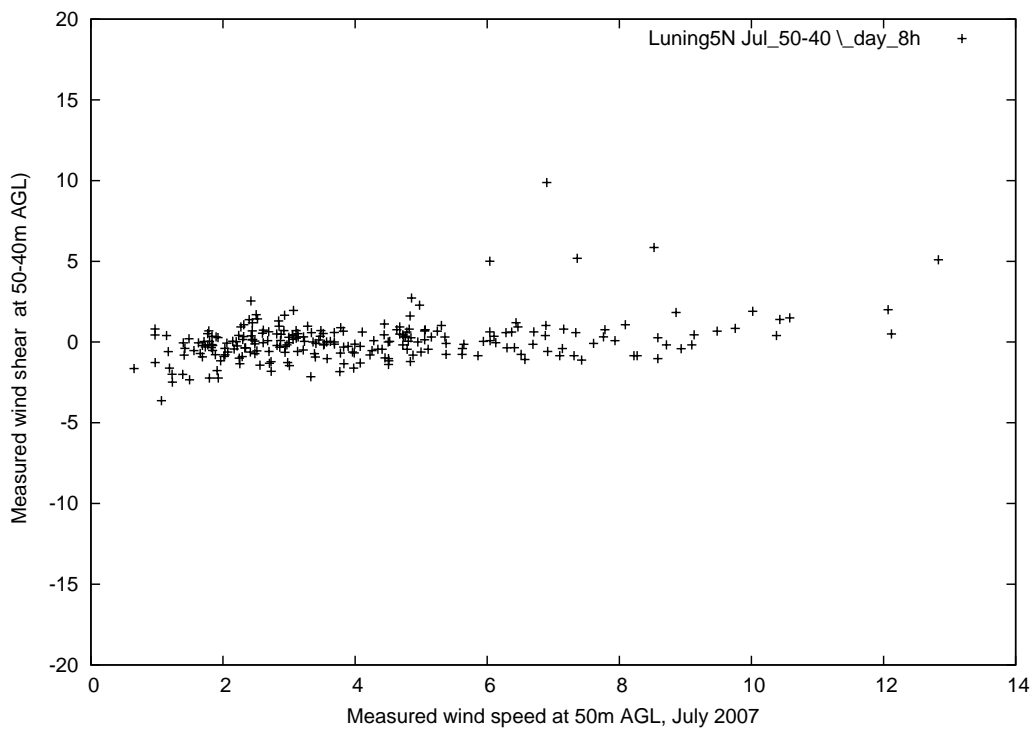


Figure 15: Scatter plots of measured wind shear between 50 m and 40 m AGL versus measured wind speed at 50 m AGL during daytime (top) and nighttime (bottom) for July 2007 at station Luning 5N.

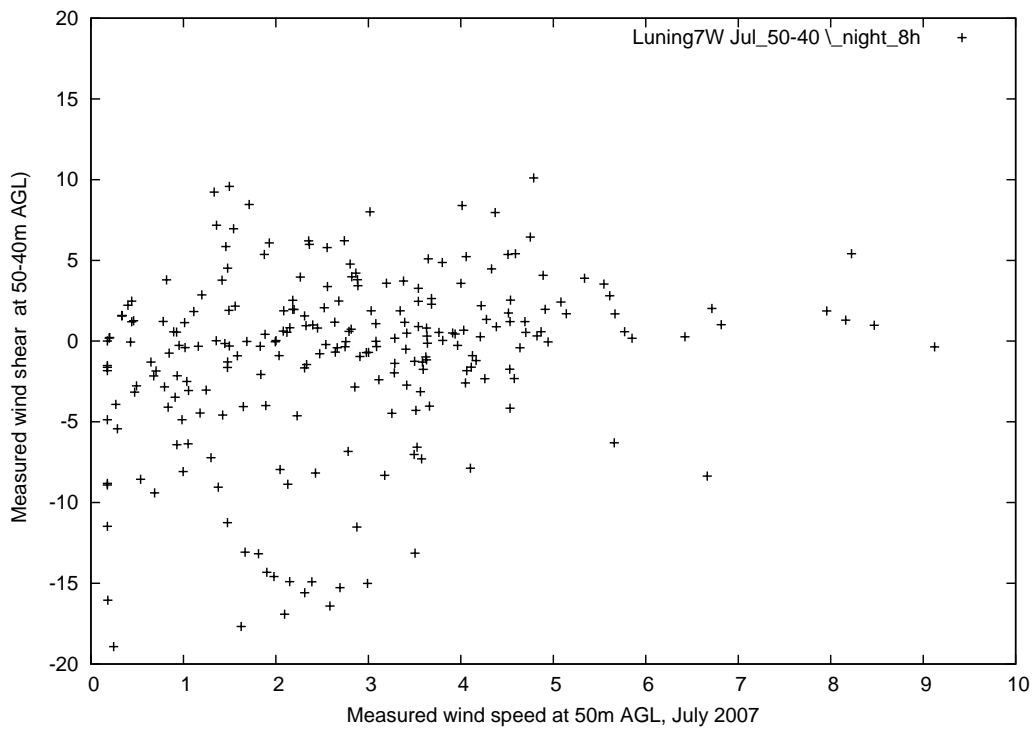
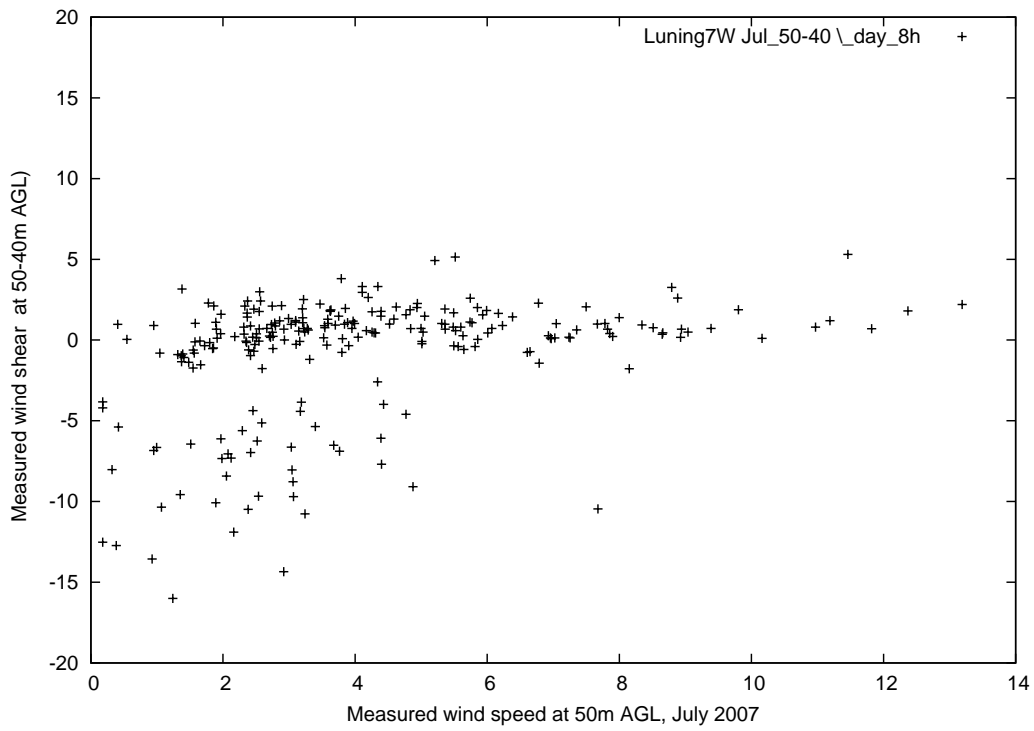


Figure 16: Scatter plots of measured wind shear between 50 m and 40 m AGL versus measured wind speed at 50 m AGL during daytime (top) and nighttime (bottom) for July 2007 at station Luning 7W.

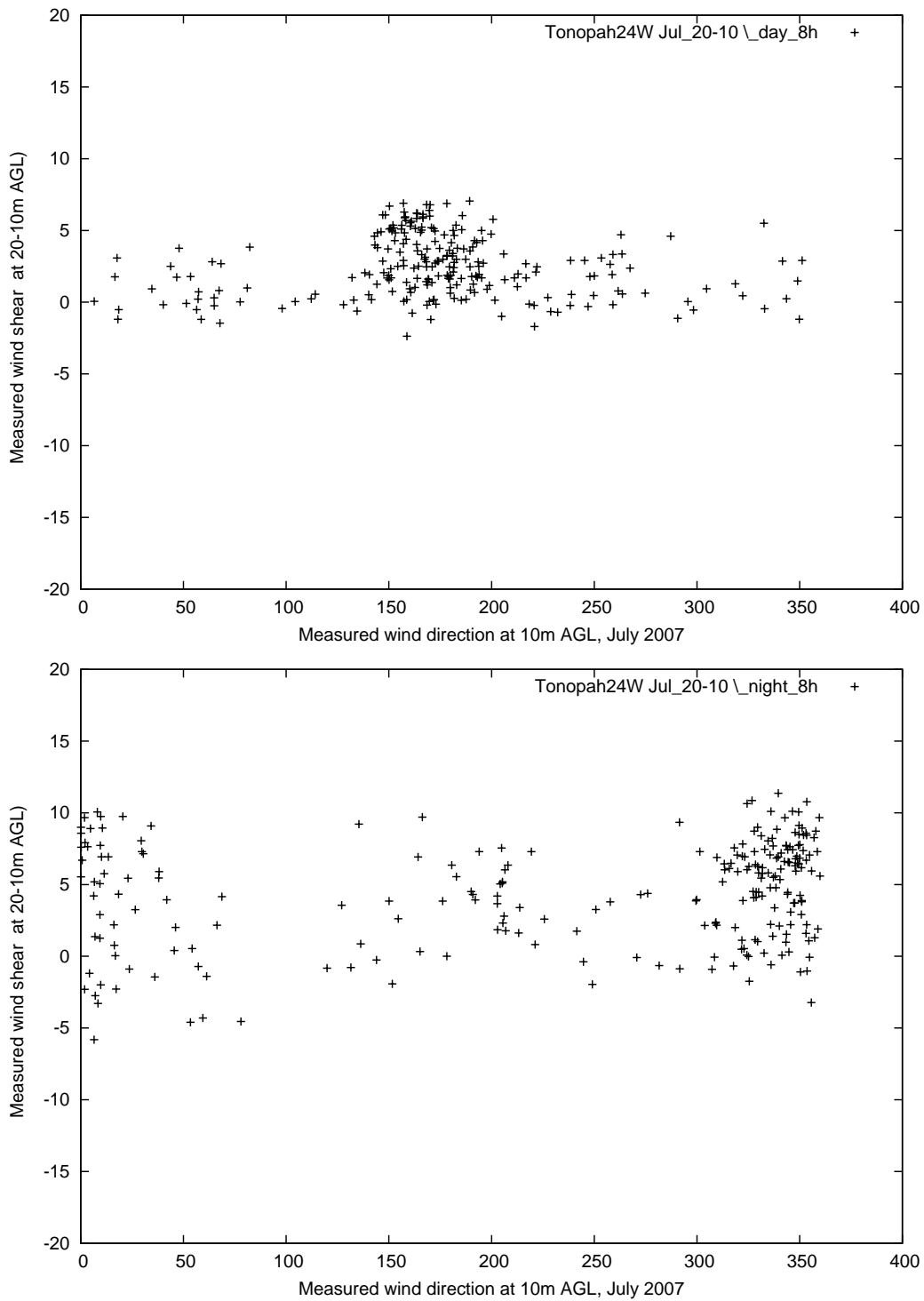


Figure 17: Scatter plots of measured wind shear between 20 m and 10 m AGL versus measured wind direction at 10 m AGL during daytime (top) and nighttime (bottom) for July 2007 at station Tonopah.

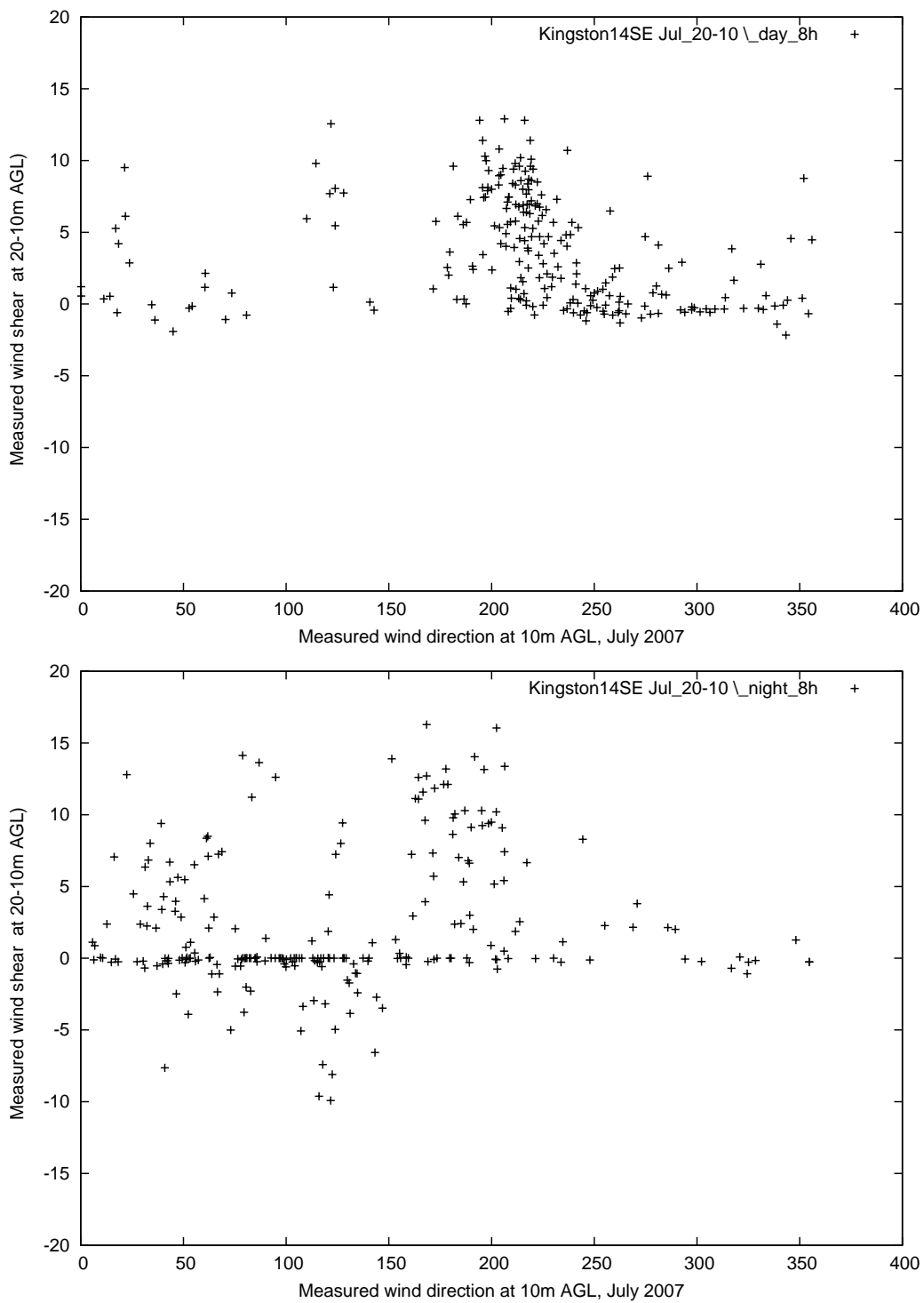


Figure 18: Scatter plots of measured wind shear between 20 m and 10 m AGL versus measured wind direction at 10 m AGL during daytime (top) and nighttime (bottom) for July 2007 at station Kingston.

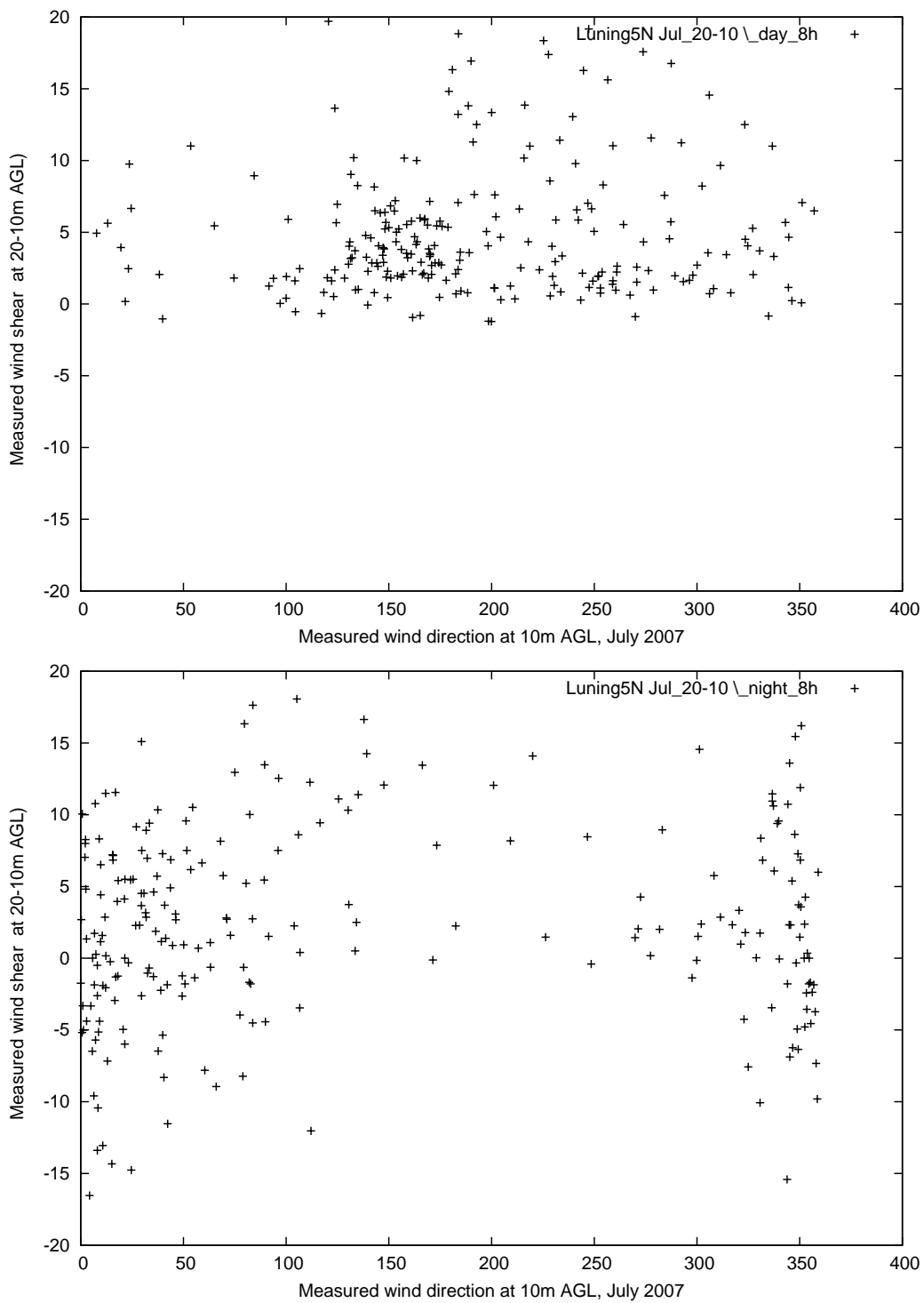


Figure 19: Scatter plots of measured wind shear between 20 m and 10 m AGL versus measured wind direction at 10 m AGL during daytime (top) and nighttime (bottom) for July 2007 at station Luning 5N.

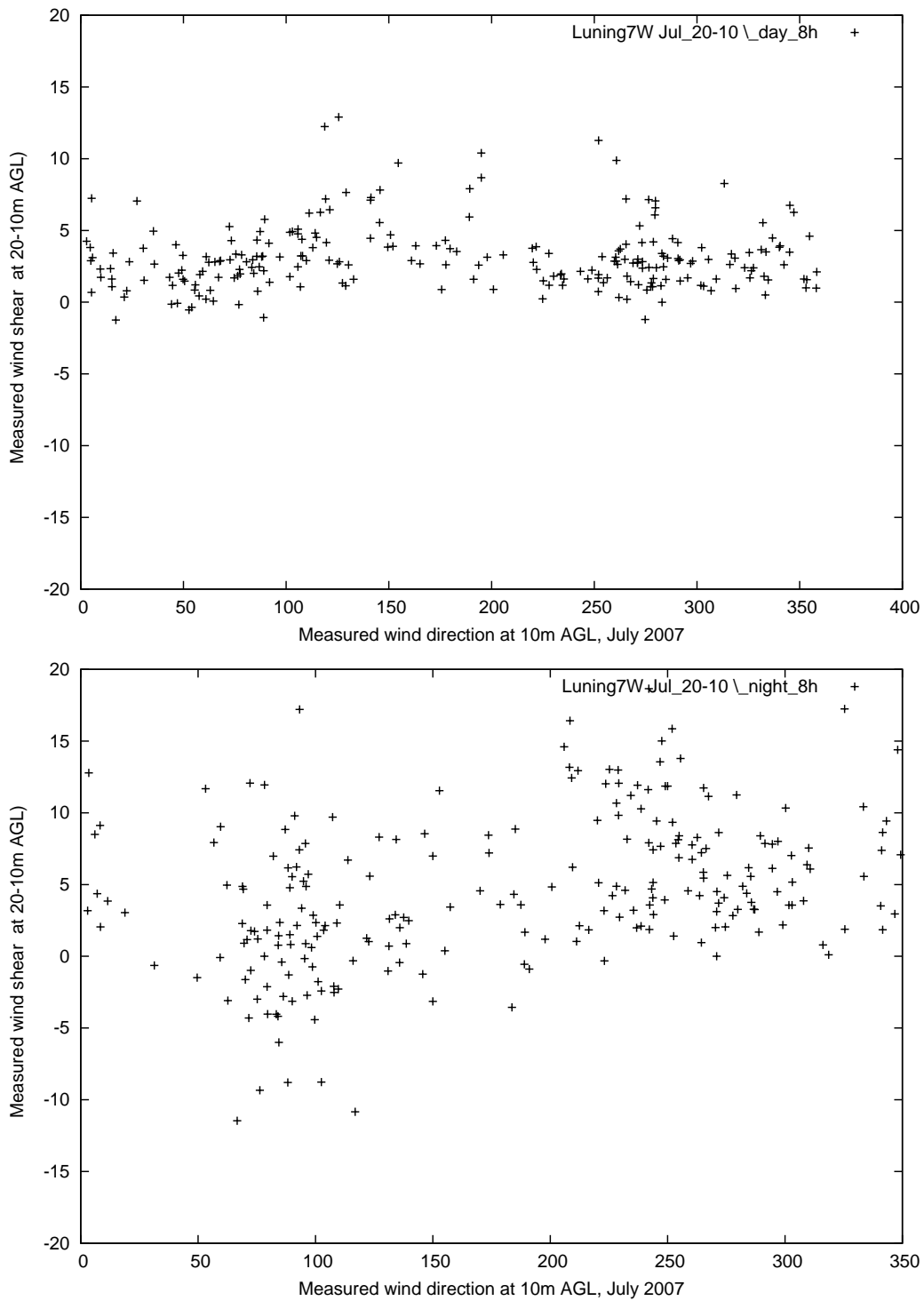


Figure 20: Scatter plots of measured wind shear between 20 m and 10 m AGL versus measured wind direction at 10 m AGL during daytime (top) and nighttime (bottom) for July 2007 at station Luning 7W.

III. Preliminary analysis of mesoscale models performance in physical space

The effect of horizontal grid resolution on the prediction accuracy of wind shear at the standard as well as hub heights (50 m AGL) was performed using two models, Mesoscale Model 5 (MM5) and Weather Research and Forecasting Model (WRF). The models are configured with nine domains, with the first four having grid resolutions 27, 9, 3 and 1 km, respectively, as well as five innermost domains at 333 m horizontal grid resolutions, with an hourly output. Four meteorological towers in central western Nevada, equipped with conventional anemometers at heights of 10 m, 20 m, 30 m, 40 m and 50 m AGL were used for evaluation of the simulated low-level wind shear and flow properties. These measurements were studied as a preparatory study, enabling the development of analysis and evaluation methodology prior to collection of newly deployed measurements envisaged by the project.

The MM5 and WRF model setups are made as similar as possible. The models were configured with seven domains; four of them having horizontal grid spacings 27 km (parent domain; referred to as 'dmn1'), 9 km ('dmn2'), 3 km ('dmn3') and 1 km ('dmn4'), respectively. Nested into the 1 km gridded domain were 3 domains (here together referred to as 'dmn5') whose horizontal grid spacing is 333 m (Figure 21). The number of vertical levels was 37 with the lowest model level set at approximately 10 m AGL. Similar combinations of the physical parameterizations were chosen for WRF and MM5: (i) the Mellor-Yamada-Janjic scheme (1.5-order turbulence closure model) to parametrize the turbulence in the planetary boundary layer (ii) Kain-Fritsch scheme (dmn1 and dmn2 only) to represent convective processes (iii) Eta surface layer scheme following Monin-Obhukov similarity theory (iv) the Dudhia [1989] scheme for shortwave radiation and the Rapid Radiative Transfer Model for longwave radiation. For the microphysics, the Reisner type of explicit microphysics is used in MM5, while the Thompson microphysics is used in WRF, which is a modified version of Reisner's microphysics. To simulate the vertical transport of soil moisture and heat, the Noah land-surface model was used in WRF and a 5-layer slab model in MM5.

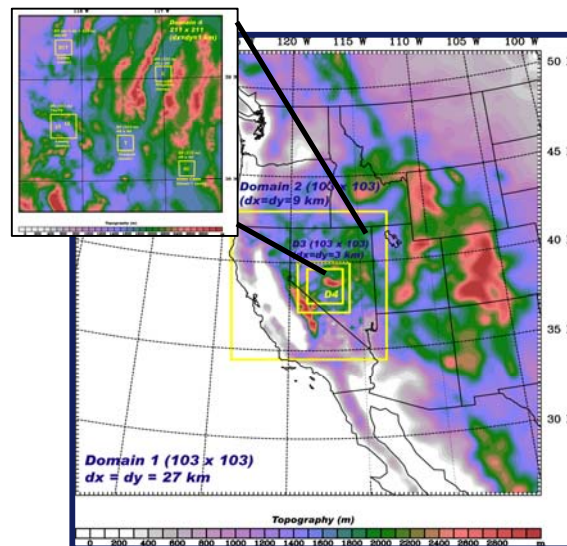


Figure 21: The model domains (dx=27km, 9 km, 3 km, 1 km, 0.3333km) used for both WRF and MM5 model simulations.

The static lower boundary conditions, *viz.* topography and land use, were interpolated from the U.S. Geological Survey datasets from an arc resolution of 10' for dmn1, 5' for dmn2 and 30" for all other domains. It should be mentioned that the terrain height at the tower locations differs across the domains. The largest differences are found in dmn1, where the elevations are overestimated by 272 m (TO), 446 m (KI), 192 m (L5) and 354 m (L7), or 316 m on average. The average difference is halved in dmn2 (153 m), further reduced in dmn3 (35 m) and almost nonexistent in dmn4 and dmn5 (< 3 m). This overestimation of terrain height at the tower locations in the lower-resolution domains is caused by the proximity of the high and steep orography of the Inyo and Sierra Mountains to the east, and one should bear in mind that larger differences are likely to affect the model verification results.

Initial and boundary conditions were provided by the three-hourly North American Regional Reanalysis (NARR). The nesting strategy of the modeling domains was one-way, using a four-point relaxation zone. The models were initialized daily at 1200 UTC to allow for a spin-up period of 12 hours in the simulation. The output data were archived with a 60-min frequency. Daily initialization, although more computationally demanding, was chosen rather than less-frequent initialization or continuous simulation.

Observed and modeled wind shear between 50 m and 10 m AGL at 4 meteorological wind towers were preliminarily analyzed with the use of measured and modeled time-series extracted from MM5 simulations (Figures 22-25). Modeled time series analyzed were extracted from model domains at 5 differing resolutions spanning from grid spacing of 27 km to 333 m. Results from domains D01 (27 km grid spacing), D02 (9 km grid spacing) and D03 (3 km grid spacing) considerably underestimate the wind shear variability and can not be considered not even partially successful in simulating the observed wind shear. In contrast, the wind shear variability is strongly enhanced in D04 (1 km grid spacing) and D05 (333 m grid spacing) and to the first approximation corresponds to the observed variability, at least for positive wind shear variability. In contrast, the intensity and variability of negative wind shear is strongly underestimated for all four wind towers. This suggests that the ability of the MM5 model to represent the negative near-surface wind shear and its variability is highly limited. Most of the negative wind shear events take place during stably stratified nocturnal conditions. This indicates that mixing in Mellor-Yamada PBL scheme might be excessive stable nocturnal conditions. This indeed is found in several other studies, where mixing for flows with larger Richardson numbers is found too diffusive, in order to keep the model numerically stable.

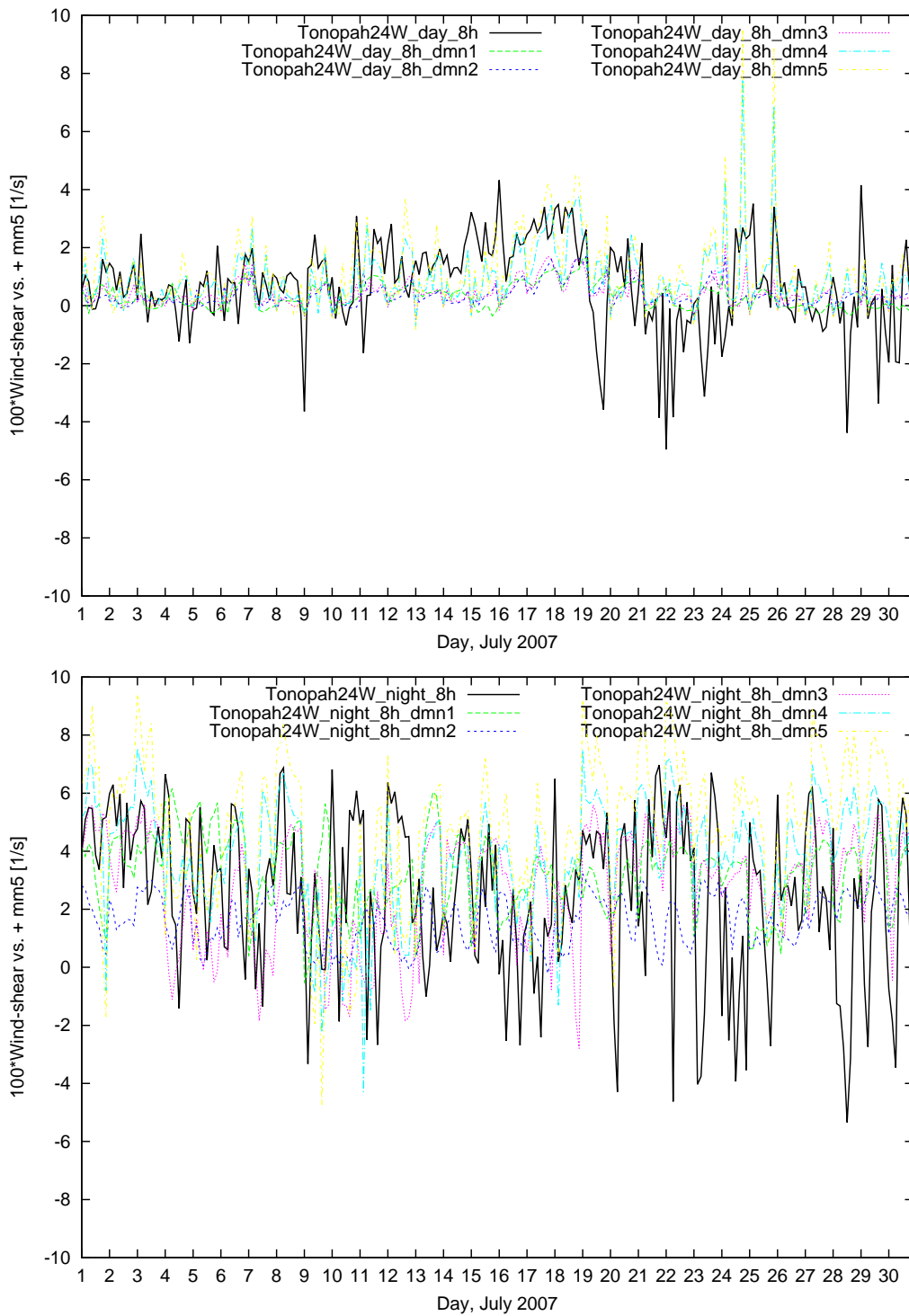


Figure 22. Observed and MM5 time series of wind shear during daytime (top) and nighttime (bottom) during July 2007 for Tonopah. MM5 data includes five domains with different grid spacing ranging from 27 km to 333 m.

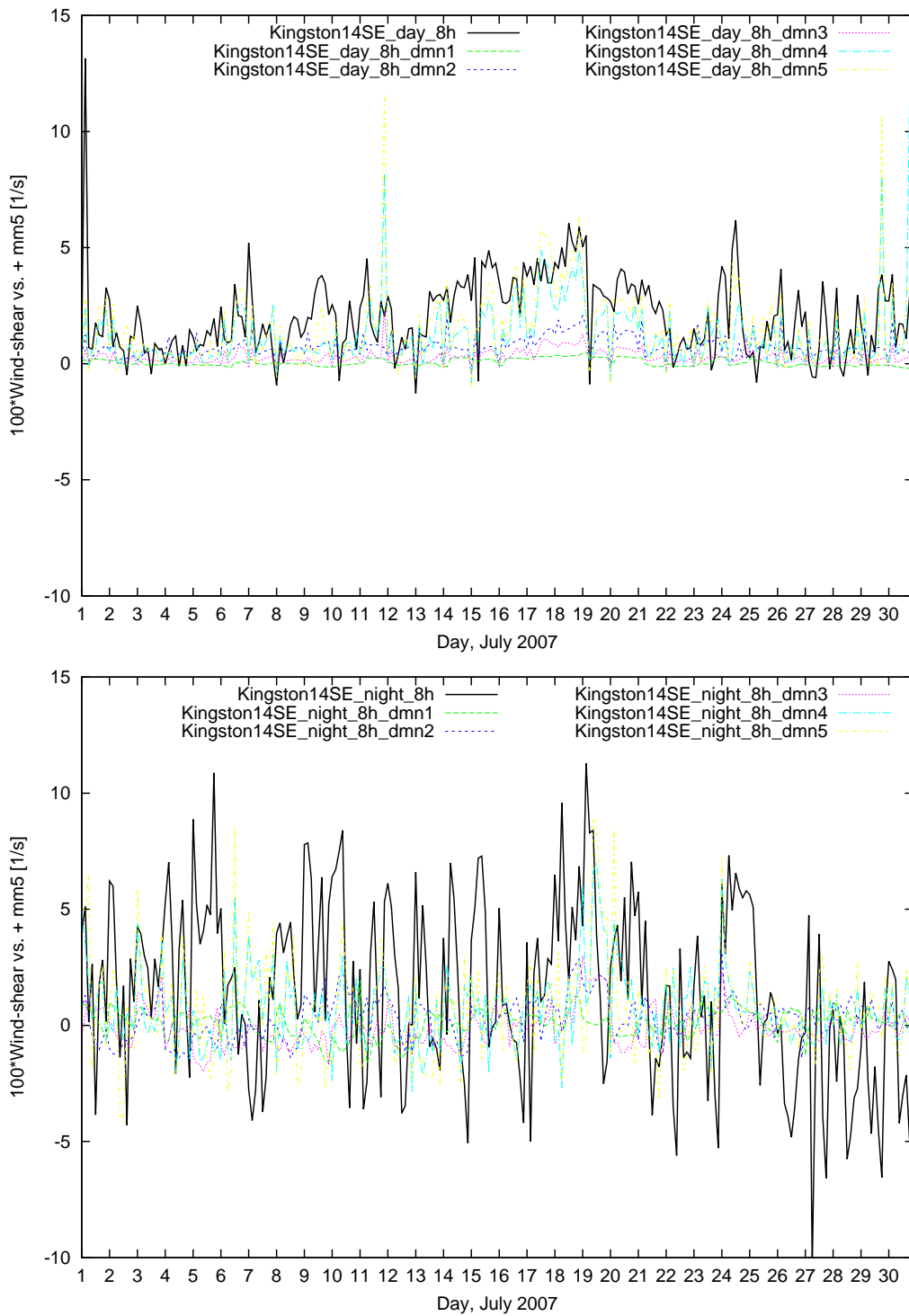


Figure 23. Observed and MM5 time series of wind shear during daytime (top) and nighttime (bottom) during July 2007 for Kingston. MM5 data includes five domains with different grid spacing ranging from 27 km to 333 m.

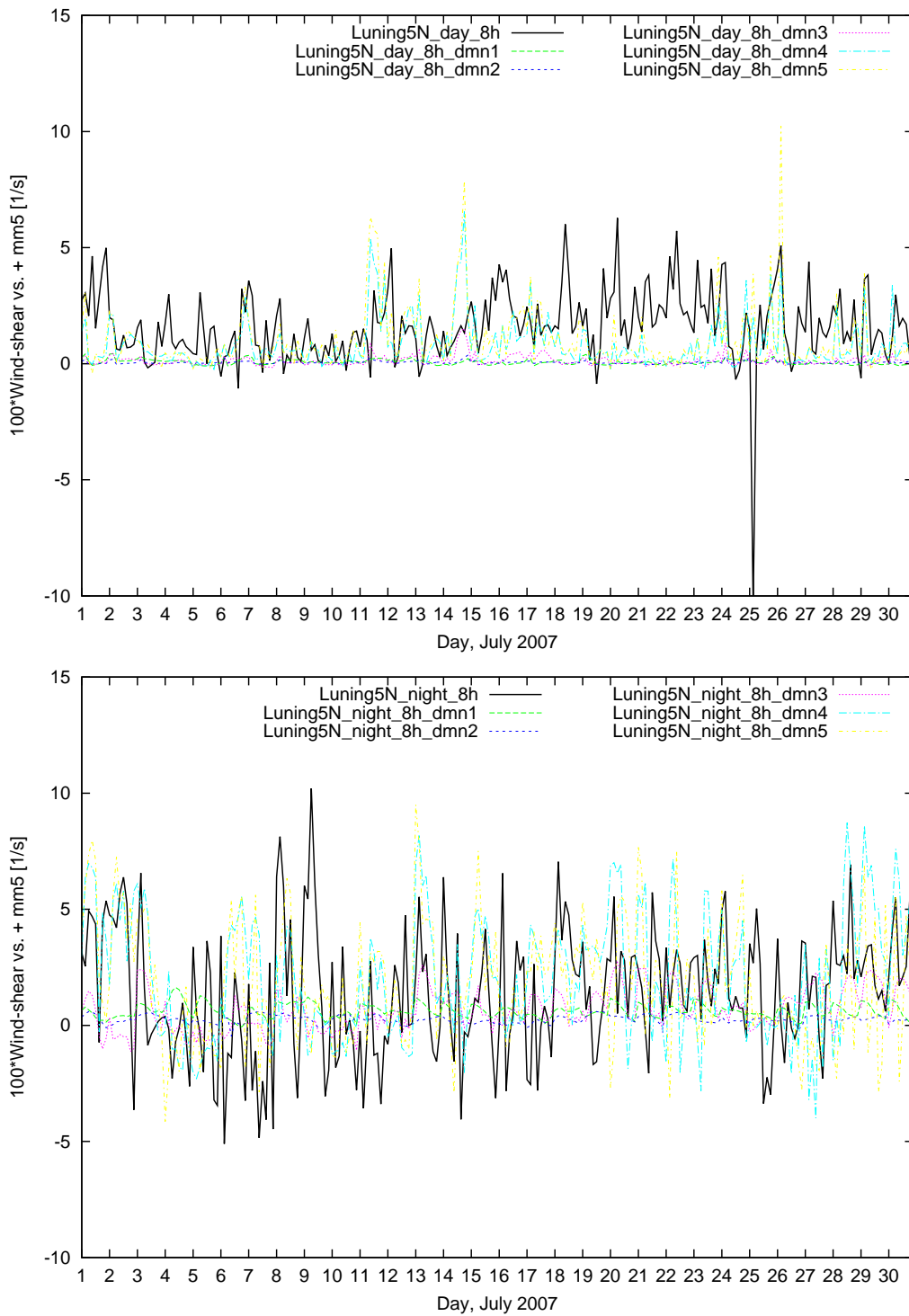


Figure 24. Observed and MM5 time series of wind shear during daytime (top) and nighttime (bottom) during July 2007 for Luning 5N. MM5 data includes five domains with different grid spacing ranging from 27 km to 333 m.

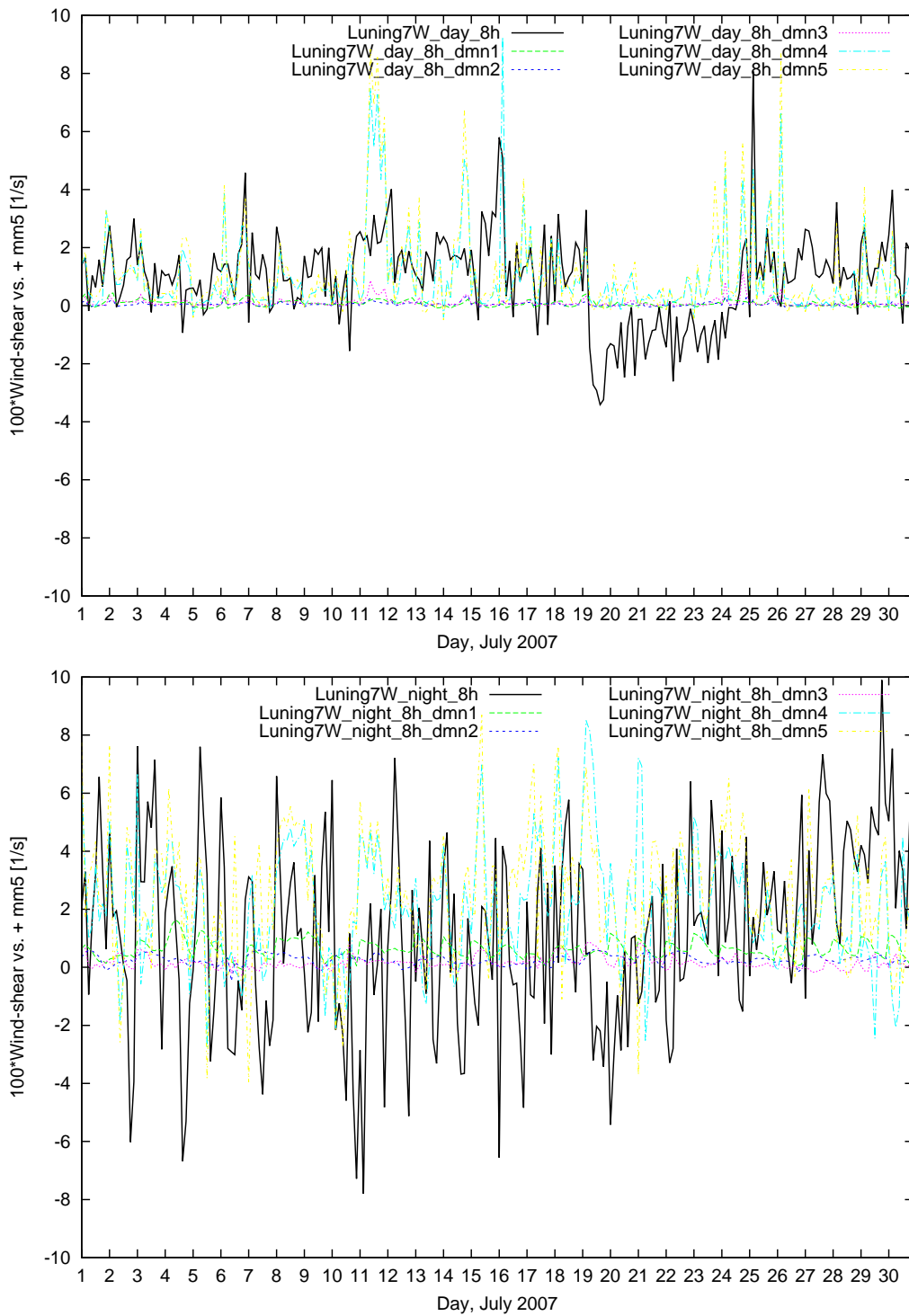


Figure 25. Observed and MM5 time series of wind shear during daytime (top) and nighttime (bottom) during July 2007 for Luning 7W. MM5 data includes five domains with different grid spacing ranging from 27 km to 333 m.

Further work

Further work will enhance observational analysis by studying wind shear distributions and spectral properties of wind shear. The analysis will be extended to December and to directional wind shear. The extensive mesoscale model evaluation will include both MM5 and WRF simulations. The moment-based and spectral verification methodology will be related to work published in Horvath et al. (2012) and adopted to account for specific wind shear properties found during the analysis. Authors plan to submit extended analysis to several conference contributions (first on International Conference on Alpine Meteorology in June 2013) and publish results in a peer-review paper.

Acknowledgement

We appreciate the comments and suggestions by Dennis Elliot (NREL) that helped to improve the report and shape directions for future work.

References

- Belu R., and D. Koračin (2009), Wind characteristics and wind energy potential in western Nevada, *Renew. Energy*, *34*, 2246–2251.
- Horvath K., D. Koračin, R. Vellore, R. Belu and J. Jiang, 2012: Sub-kilometer dynamical downscaling of near-surface winds in complex terrain using WRF and MM5 mesoscale models. *J. Geophys. Res.*, **117**, D11111, 19pp., doi:10.1029/2012JD017432.
- Skamarock, W. C., 2004: Evaluating Mesoscale NWP Models Using Kinetic Energy Spectra. *Mon. Wea. Rev.*, **132**, 3019-3032.